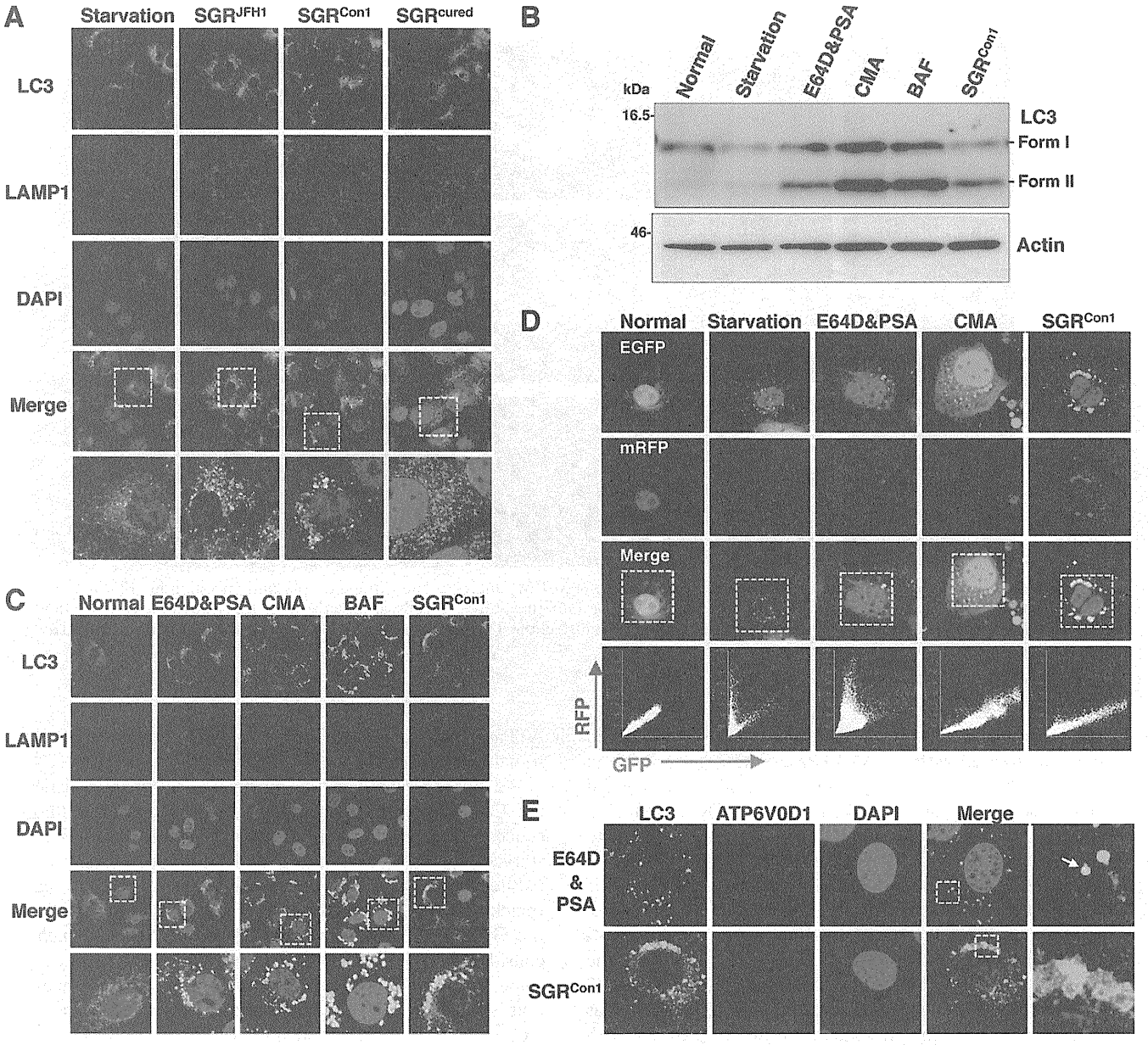

FIG. 3. Inhibition of autophagy maturation in HCV replicon cells. (A) After nuclear staining with DAPI, starved Huh7 cells, replicon cells, and SGR^{cured} cells were stained with rabbit polyclonal anti-LC3 and mouse monoclonal anti-LAMP1 antibodies followed by Alexa Fluor 488- and 594-conjugated secondary antibodies, respectively, and examined by confocal microscopy. The boxed regions in the merged images are magnified. (B and C) Huh7 cells were treated with 20 μM protease inhibitors (E64D and PSA) or a 20 nM concentration of a V-ATPase inhibitor (CMA or BAF) for 6 h. (B) Cell lysates were subjected to immunoblotting using antibodies against LC3 and β-actin. (C) Intracellular localization of LAMP1 and LC3 was determined by confocal microscopy after staining with DAPI and appropriate antibodies. The boxed areas in the merged images are magnified. (D) Tandem fluorescence-tagged LC3 assay. The expression plasmid encoding mRFP-GFP-tandem-tagged LC3 was transfected into naïve and starved Huh7 cells or into the SGR^{Con1} cells treated with the indicated inhibitors at 36 h posttransfection. The resulting cells were fixed at 42 h posttransfection, and the relative GFP and RFP signals were determined by confocal microscopy. The fluorescent values in the boxes of the merged images were determined and shown as dot plots in the bottom column of the grid, in which the *x* and *y* axes indicate the signals of GFP and RFP, respectively. (E) Huh7 cells treated with E64D and PSA and the SGR^{Con1} cells were stained with DAPI and then with rabbit polyclonal anti-LC3 and mouse monoclonal anti-ATP6V0D1 antibodies followed by Alexa Fluor 488- and 594-conjugated secondary antibodies, respectively. The boxed regions in the merged images are magnified. A white arrow indicates colocalization of LC3 and ATP6V0D1. The data shown are representative of three independent experiments.

drolases in the vesicle (2). Next, to determine the possibility of a deficiency in the acidification of the autolysosome on the autophagic dysfunction in the Con1 replicon cells, Huh7 cells were treated with the protease inhibitors E64D and pepstatin A (PSA) or with each of the V-ATPase inhibitors concanamycin A (CMA) and bafilomycin A1 (BAF). The amount of LC3-II was significantly increased in Huh7 cells treated with the inhibitors just as in the SGR^{Con1} cells (Fig. 3B). Further-

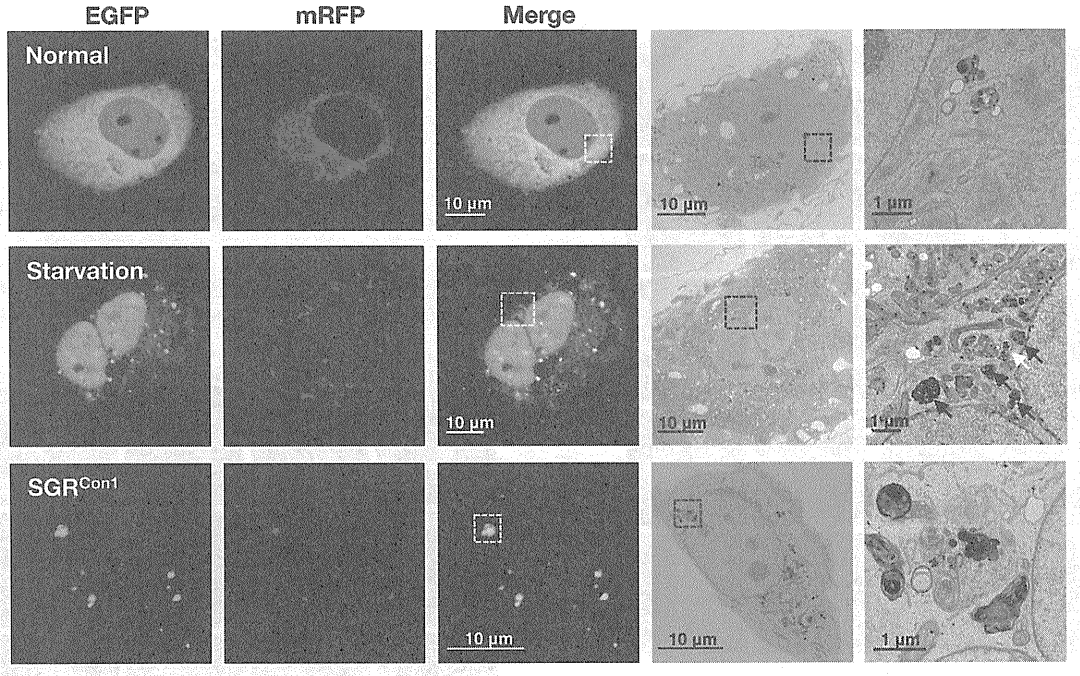

FIG. 4. Correlative fluorescence microscopy-electron microscopy (FM-EM) analysis. The expression plasmid encoding mRFP-GFP-tandem-tagged LC3 was transfected into naïve and starved Huh7 cells or into the SGR^{Con1} cells as described in the legend to Fig. 3D, and the mRFP-GFP-tandem-tagged LC3 signals were observed at 36 h posttransfection. The boxed regions in the merged images are magnified. The data shown are representative of three independent experiments.

more, the large foci of LC3 colocalized with LAMP1 appeared in the cells treated with the V-ATPase inhibitors, as seen in SGR^{Con1} cells (Fig. 3C). These results suggest that stacked autophagosome flux caused by the inhibition of lysosomal degradation or acidification exhibits characteristics similar to those observed in the Con1 replicon cells.

Since the fluorescence of GFP but not that of monomeric red fluorescent protein (mRFP) disappears under the acidic environment, expression of mRFP-GFP tandem fluorescent-tagged LC3 (tfLC3) is capable of being used to monitor the acidic status of the autolysosome (24). Both GFP and mRFP fluorescent signals were unfused, some of them accumulated as small foci in Huh7 cells after starvation or by treatment with the protease inhibitors, and half of the foci of mRFP were not colocalized with those of GFP (Fig. 3D), indicating that half of the foci are in an acidic state due to maturation into an autolysosome after fusion with a lysosome. On the other hand, the large foci of GFP and mRFP were completely colocalized in Huh7 cells treated with CMA or in the SGR^{Con1} cells. These results suggest that the large foci of LC3 in the SGR^{Con1} cells are not under acidic conditions. Recently, it was shown that the lack of lysosomal acidification in human genetic disorders due to dysfunction in assembly/sorting of V-ATPase induces incomplete autophagy similar to that observed in SGR^{Con1} cells (31, 45). Therefore, to explore the reason for the lack of acidification of the autolysosome in the SGR^{Con1} cells, we examined the subcellular localization of ATP6V0D1, a subunit of the integral membrane V_0 complex of V-ATPase. Colocalization of ATP6V0D1 with large foci of LC3 was observed in Huh7 cells treated with the protease inhibitors but not in SGR^{Con1} cells (Fig. 3E), suggesting that dislocation of V-ATPase may participate in the impairment of the autolysosomal acidification in the SGR^{Con1} cells.

We further examined the morphological characteristics of the LC3-positive compartments by using correlative fluorescence microscopy-electron microscopy (FM-EM) (Fig. 4). The starved Huh7 cells exhibited a small double-membrane vesicle (white arrow) and high-density single-membrane structures (black arrows) in close proximity to the correlative position of the GFP- and mRFP-positive LC3 compartments, which are considered to be the autophagosome and lysosome/autolysosome, respectively. In contrast, many high-density membranous structures were detected in the correlative position of the large GFP- and mRFP-positive LC3 compartment in the SGR^{Con1} cells, which is well consistent with the observation in the time-lapse imaging in which small foci of LC3 headed toward and assembled with the large LC3-positive compartment (see movies in the supplemental material). These results suggest that the formation of large aggregates with aberrant inner structures in the SGR^{Con1} cells may impair maturation of the autolysosome through the interference of further fusion with functional lysosomes for the degradation.

The secretion of immature cathepsin B is enhanced in the replicon cell of strain Con1. Lysosomal acidification is required for the cleavage of cathepsins for activation, and cathepsin B (CTSB) is processed under acidic conditions (13). Although a marginal decrease of CTSB was detected in the whole lysates of the SGR^{Con1} cells, a significant reduction in the expression of both unprocessed (pro-CTSB) and matured CTSB was observed in the lysosomal fractions of the SGR^{Con1} cells compared with those of the naïve Huh7 and the SGR^{cured} cells (Fig. 5A). LAMP1 was concentrated at a similar level in

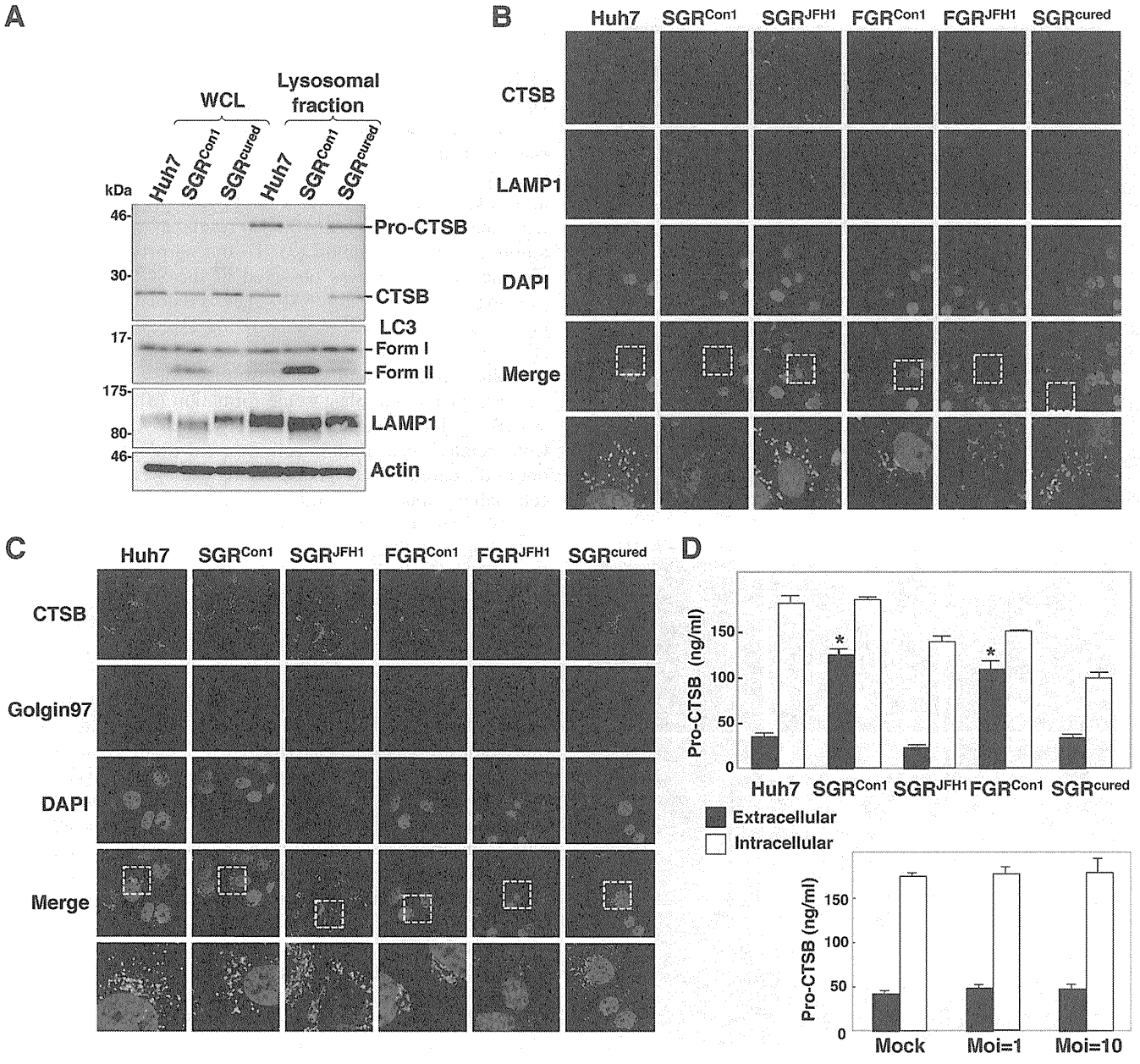

FIG. 5. Enhanced secretion of pro-CTSB in the HCV replicon cells. (A) The whole-cell lysate (WCL) and lysosomal fraction prepared from Huh7, SGR^{Con1}, and SGR^{cured} cells were subjected to immunoblotting. (B and C) Huh7 cells, HCV replicon cells, and SGR^{cured} cells were stained with DAPI, rabbit polyclonal anti-CTSB antibody, and mouse anti-LAMP1 (B) or anti-Golgin97 (C) antibody. The boxed areas in the merged images are magnified. (D) Expression of pro-cathepsin B in the culture supernatants (black bars) and cell lysates (white bars) of the Huh7, SGR^{Con1}, SGR^{JFH1}, FGR^{Con1}, and SGR^{cured} cells and the SGR^{cured} cells infected with HCVcc at a multiplicity of infection (Moi) of 1 or 10 and incubated for 72 h was determined by enzyme-linked immunosorbent assay (ELISA). The error bars indicate standard deviations. The asterisks indicate significant differences ($P < 0.01$) versus the control value. The data shown are representative of three independent experiments.

the lysosomal fractions of the cells, whereas LC-II was detected in the fractions of the SGR^{Con1} cells but not in those of Huh7 and the SGR^{cured} cells, suggesting that autophagosomes and/or autolysosomes in the SGR^{Con1} cells are fractionated in the lysosomal fraction. Colocalization of CTSB with LAMP1 was observed in the naïve Huh7 cells, in the SGR^{cured} cells, and in the replicon cells harboring a sub- or a full genomic RNA of strain JFH1 (SGR^{JFH1} and FGR^{JFH1}, respectively) but not in those of strain Con1 (SGR^{Con1} and FGR^{Con1}) (Fig. 5B). On the other hand, CTSB was colocalized with Golgin97, a marker for the Golgi apparatus, in the SGR^{Con1} and FGR^{Con1} cells but not in other cells (Fig. 5C). Since previous reports suggested that the alkalization in the lysosome triggers secretion of the unprocessed lysosomal enzymes (19, 41), we next determined the secretion of pro-CTSB in the replicon cells. Secretion of the pro-CTSB was significantly enhanced in the replicon cells of strain Con1 but not in those of strain JFH1 and naïve and cured cells (Fig. 5D, top). Furthermore, secretion of pro-CTSB

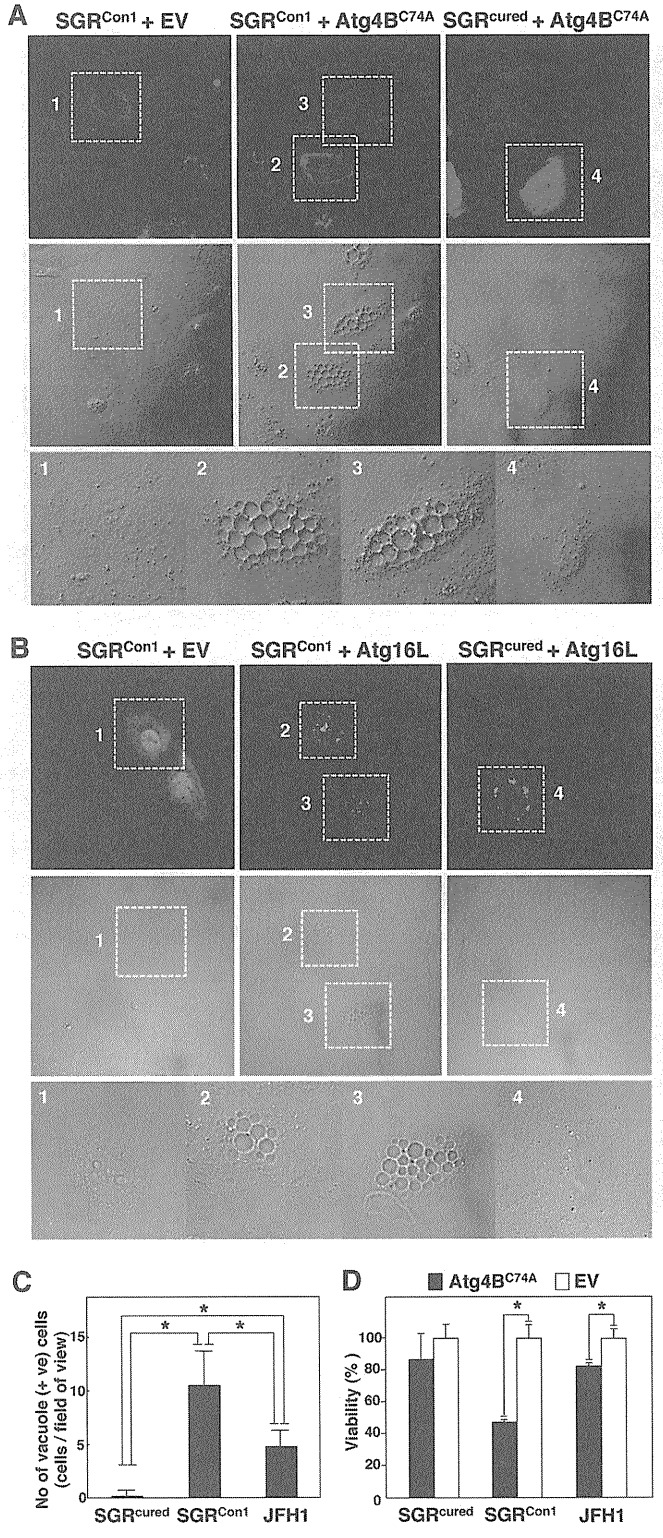

FIG. 6. Inhibition of autophagosome formation induces severe cytoplasmic vacuolations leading to cell death in the HCV replicon cells. (A) SGR^{Con1} and SGR^{cured} cells transfected with pStrawberry-$Atg4B^{C74A}$ or empty vector pStrawberry (EV) were fixed at 48 h posttransfection and examined by fluorescence microscopy. The boxed areas in the phase-contrast images are magnified. (B) SGR^{Con1} and SGR^{cured} cells transfected with pEGFP-Atg16L or EV were examined by fluorescence microscopy at 48 h posttransfection. The boxed areas in the phase-contrast images are magnified. (C) SGR^{cured}, SGR^{Con1}, and SGR^{cured} cells infected with JFH1 virus were transfected with pStrawberry-$Atg4B^{C74A}$, and the number of vacuole-positive cells in each of nine fields of view was counted at 48 h posttransfection. (D) SGR^{cured}, SGR^{Con1}, and SGR^{cured} cells infected with JFH1 virus were transfected with pStrawberry-$Atg4B^{C74A}$ (black bars) or EV (white bars), and cell viability was determined at 6 days posttransfection by using CellTiter-Glo (Promega) according to the manufacturer's protocol. The asterisks indicate significant differences ($P < 0.05$) versus the control value. The data shown are representative of three independent experiments.

was not observed in the cured cells infected with HCVcc, an infectious HCV strain derived from strain JFH1 (Fig. 5D, bottom). Collectively, these results suggest that the dysfunction of lysosomal acidification contributes to the impairment of autophagy in the HCV replicon cells of strain Con1.

Autophagy induced in cells replicating HCV is required for cell survival. Finally, we examined the pathological significance of autophagy during HCV replication. Atg4B is known as an LC3-processing protease, and overexpression of its protease-inactive mutant ($Atg4B^{C74A}$) results in inhibition of the autophagosome formation (7). To our surprise, severe cytoplasmic vacuolation was observed in the SGR^{Con1} cells expressing $Atg4B^{C74A}$ (Fig. 6A). These vacuolations were also observed in the SGR^{Con1} cells by the expression of Atg16L (Fig. 6B), a molecule that is an essential component of the autophagy complex and that, if expressed in excess amounts, can disrupt the autophagosome formation (8). Expression of $Atg4B^{C74A}$ induced a higher level of vacuole formation in the Con1 replicon cells than in cells infected with JFH1 virus but not in the cured cells (Fig. 6C). Along with these vacuolations, cell viability was significantly decreased by the expression of $Atg4B^{C74A}$ in SGR^{Con1} cells and slightly in JFH1 virus-infected cells (Fig. 6D). These results suggest that autophagy induced by the RNA replication of HCV is required for host cell survival.

DISCUSSION

In the present study, we demonstrated that two genotypes of HCV induce autophagy, whereas intact autophagy flux is required for the host cell to survive. The cell death characterized by cytoplasmic vacuolation that was induced in the HCV replicon cells by the inhibition of the autophagosome formation is similar to type III programmed cell death, which is distinguishable from apoptosis and autophagic cell death (4). Type III programmed cell death has been observed in the neurodegenerative diseases caused by the deposit of cytotoxic protein aggregates (15).

We previously reported that HCV hijacks chaperone complexes, which regulates quality control of proteins into the membranous web for circumventing unfolded protein response during efficient genome replication (53); in other words, the replication of HCV exacerbates the generation of proteins associated with cytotoxicity. In the experiments using a chimpanzee model, HCV of genotype 1 was successfully used to reproduce acute and chronic hepatitis similar to that in the human patients (3, 57), and transgenic mice expressing viral proteins of HCV of genotype 1b have been shown to develop

Sjögren syndrome, insulin resistance, hepatic steatosis, and hepatocellular carcinoma (27, 28). In contrast, HCVcc, based on the genotype 2a strain JFH1 isolated from a patient with fulminant hepatitis C (33, 56), was unable to establish chronic infection in chimpanzees (56) or to induce cell damage and inflammation in chimeric mice xenotransplanted with human hepatocytes (17). These results imply that the onset of HCV pathogenesis could be dependent not only upon an amount but also on a property of deposited proteins, and they might explain the aggravated vacuolations under the inhibition of autophagosome formation in strain Con1 compared to that in strain JFH1. Interestingly, the overexpression of $Atg4B^{C74A}$ or Atg16L causes eccentric cell death in the Con1 replicon cells in which autophagy flux is already disturbed. Thus, we speculated that the quarantine of undefined abnormalities endowed with high cytotoxicity by the engulfing of the autophagic membrane might be sufficient for the amelioration of HCV-induced degeneration. The autophagosomal dysfunction observed in the Con1 replicon cells may suggest that a replicant of strain Con1 was more sensitive to the lysosomal vacuolation than that of strain JFH1. Because a limitation of our study was that we were unable to use infectious HCV of other strains, it is still unclear whether the autophagic degradation can be impaired only in the replicon of HCV strain Con1 or genotype 1.

We also demonstrated that HCV replication of strain Con1 but not that of strain JFH1 facilitates the secretion of pro-CTSB. It has been well established that the secretion of pro-CTSB is enhanced in several types of tumors (26, 50). The secretion of CTSB, like the secretion of matrix metalloproteases, is a marker of the progression of the proteolytic degradation of the extracellular matrix, which plays an important part in cancer invasion and metastasis. Since infection with HCV of genotype 1 is clinically considered a risk factor for the development of hepatocellular carcinoma (14, 51), the enhanced secretion of pro-CTSB by the replication of genotype 1 strains might synergistically promote infiltration of hepatocellular carcinoma.

As shown elsewhere (see movies in the supplemental material), although most degradations of the autophagosome were impaired due to a dislocalization of a V-ATPase subunit, some autophagic degradation was achieved in the SGR^{Con1} cells similar to that in the starved Huh7 cells. Moreover, the stagnated autophagy flux was rescued by the treatment of alpha interferon accompanied by elimination of HCV (Fig. 1C and D). Interestingly, we observed neither a significant impairment of lysosomal degradation nor the intracellular activity of cathepsins in the replicon cells of HCV strain Con1 (data not shown). Therefore, there might be a specific dysfunction within the autolysosome during the replication of HCV strain Con1. Detailed studies are needed to elucidate how HCV strain Con1 disturbs the sorting of V-ATPase.

A close relationship between autophagy and the immune system has been gradually unveiled (47). Autophagy assists not only in the direct elimination of pathogens by hydrolytic degradation but also in antigen processing in antigen-presenting cells such as macrophage and dendritic cells (DC) for presentation by major histocompatibility complex (MHC) I and II (11). Moreover, autophagy plays important roles in T lymphocyte homeostasis (44). As such, in some instances, interruptions of autophagy can allow microorganisms to escape from the host immune system. Indeed, the immune response against herpes simplex virus was suppressed by blocking the autophagy (6). With regard to HCV, functionally impaired DC dysfunctions marked by poor DC maturation, impaired antigen presentation, and attenuated cytokine production have been reported in tissue culture models and chronic hepatitis C patients (1, 22, 46). In addition, reduction of cell surface expression of MHC-I in HCV genotype 1b replicon cells has been reported (55). We confirmed that levels of cell surface expression of MHC-I in the replicon cells of genotype 1b, but not of genotype 2a, were reduced in comparison with those in the cured cells (data not shown). Hence it might be feasible to speculate that the replication of HCV RNA of genotype 1 induces an incomplete autophagy for attenuating antigen presentation to establish persistent infection. In contrast, autophagy is known to serve as a negative regulator of innate immunity (21, 54). A recent report demonstrated that autophagy induced by infection with strain JFH1 or dengue virus attenuates innate immunity to promote viral replication (23), indicating that an HCV genotype 2a strain may facilitate autophagy to evade innate immunity.

In this study, we demonstrated that HCV utilizes autophagy to circumvent the cell death induced by vacuole formation for its survival. This unique strategy of HCV propagation may provide new clues to the virus-host interaction and, ultimately, to the pathogenesis of infection by various genotypes of HCV.

ACKNOWLEDGMENTS

We thank H. Murase and M. Tomiyama for their secretarial work. We also thank R. Bartenschlager and T. Wakita for providing cell lines and plasmids.

This work was supported in part by grants-in-aid from the Ministry of Health, Labor, and Welfare (Research on Hepatitis), the Ministry of Education, Culture, Sports, Science, and Technology, and the Osaka University Global Center of Excellence Program.

REFERENCES

1. **Auffermann-Gretzinger, S., E. B. Keeffe, and S. Levy.** 2001. Impaired dendritic cell maturation in patients with chronic, but not resolved, hepatitis C virus infection. Blood **97:**3171–3176.
2. **Beyenbach, K. W., and H. Wieczorek.** 2006. The V-type H+ ATPase: molecular structure and function, physiological roles and regulation. J. Exp. Biol. **209:**577–589.
3. **Bradley, D. W.** 2000. Studies of non-A, non-B hepatitis and characterization of the hepatitis C virus in chimpanzees. Curr. Top. Microbiol. Immunol. **242:**1–23.
4. **Clarke, P. G.** 1990. Developmental cell death: morphological diversity and multiple mechanisms. Anat. Embryol. (Berl.) **181:**195–213.
5. **Dreux, M., P. Gastaminza, S. F. Wieland, and F. V. Chisari.** 2009. The autophagy machinery is required to initiate hepatitis C virus replication. Proc. Natl. Acad. Sci. U. S. A. **106:**14046–14051.
6. **English, L., et al.** 2009. Autophagy enhances the presentation of endogenous viral antigens on MHC class I molecules during HSV-1 infection. Nat. Immunol. **10:**480–487.
7. **Fujita, N., et al.** 2008. An Atg4B mutant hampers the lipidation of LC3 paralogues and causes defects in autophagosome closure. Mol. Biol. Cell **19:**4651–4659.
8. **Fujita, N., et al.** 2008. The Atg16L complex specifies the site of LC3 lipidation for membrane biogenesis in autophagy. Mol. Biol. Cell **19:**2092–2100.
9. **Fujitani, Y., C. Ebato, T. Uchida, R. Kawamori, and H. Watada.** 2009. β-cell autophagy: a novel mechanism regulating β-cell function and mass: lessons from β-cell-specific Atg7-deficient mice. Islets **1:**151–153.
10. **Gannage, M., et al.** 2009. Matrix protein 2 of influenza A virus blocks autophagosome fusion with lysosomes. Cell Host Microbe **6:**367–380.
11. **Gannage, M., and C. Munz.** 2009. Autophagy in MHC class II presentation of endogenous antigens. Curr. Top. Microbiol. Immunol. **335:**123–140.
12. **Hara, T., et al.** 2006. Suppression of basal autophagy in neural cells causes neurodegenerative disease in mice. Nature **441:**885–889.
13. **Hasilik, A.** 1992. The early and late processing of lysosomal enzymes: proteolysis and compartmentation. Experientia **48:**130–151.

14. **Hatzakis, A., et al.** 1996. Hepatitis C virus 1b is the dominant genotype in HCV-related carcinogenesis: a case-control study. Int. J. Cancer **68:**51–53.
15. **Hirabayashi, M., et al.** 2001. VCP/p97 in abnormal protein aggregates, cytoplasmic vacuoles, and cell death, phenotypes relevant to neurodegeneration. Cell Death Differ. **8:**977–984.
16. **Hiraga, N., et al.** 2011. Rapid emergence of telaprevir resistant hepatitis C virus strain from wildtype clone in vivo. Hepatology (Baltimore, Md.) **54:**781–788.
17. **Hiraga, N., et al.** 2007. Infection of human hepatocyte chimeric mouse with genetically engineered hepatitis C virus and its susceptibility to interferon. FEBS Lett. **581:**1983–1987.
18. **Ichimura, Y., E. Kominami, K. Tanaka, and M. Komatsu.** 2008. Selective turnover of p62/A170/SQSTM1 by autophagy. Autophagy **4:**1063–1066.
19. **Isidoro, C., et al.** 1995. Altered intracellular processing and enhanced secretion of procathepsin D in a highly deviated rat hepatoma. Int. J. Cancer **60:**61–64.
20. **Jacobson, I. M., P. Cacoub, L. Dal Maso, S. A. Harrison, and Z. M. Younossi.** 2010. Manifestations of chronic hepatitis C virus infection beyond the liver. Clin. Gastroenterol. Hepatol. **8:**1017–1029.
21. **Jounai, N., et al.** 2007. The Atg5 Atg12 conjugate associates with innate antiviral immune responses. Proc. Natl. Acad. Sci. U. S. A. **104:**14050–14055.
22. **Kanto, T., et al.** 1999. Impaired allostimulatory capacity of peripheral blood dendritic cells recovered from hepatitis C virus-infected individuals. J. Immunol. **162:**5584–5591.
23. **Ke, P. Y., and S. S. Chen.** 2011. Activation of the unfolded protein response and autophagy after hepatitis C virus infection suppresses innate antiviral immunity in vitro. J. Clin. Invest. **121:**37–56.
24. **Kimura, S., N. Fujita, T. Noda, and T. Yoshimori.** 2009. Monitoring autophagy in mammalian cultured cells through the dynamics of LC3. Methods Enzymol. **452:**1–12.
25. **Kiyosawa, K., et al.** 1990. Interrelationship of blood transfusion, non-A, non-B hepatitis and hepatocellular carcinoma: analysis by detection of antibody to hepatitis C virus. Hepatology **12:**671–675.
26. **Koblinski, J. E., et al.** 2002. Interaction of human breast fibroblasts with collagen I increases secretion of procathepsin B. J. Biol. Chem. **277:**32220–32227.
27. **Koike, K., et al.** 1997. Sialadenitis histologically resembling Sjogren syndrome in mice transgenic for hepatitis C virus envelope genes. Proc. Natl. Acad. Sci. U. S. A. **94:**233–236.
28. **Koike, K., T. Tsutsumi, H. Yotsuyanagi, and K. Moriya.** 2010. Lipid metabolism and liver disease in hepatitis C viral infection. Oncology **78**(Suppl. 1)**:**24–30.
29. **Komatsu, M., et al.** 2006. Loss of autophagy in the central nervous system causes neurodegeneration in mice. Nature **441:**880–884.
30. **Komatsu, M., et al.** 2007. Homeostatic levels of p62 control cytoplasmic inclusion body formation in autophagy-deficient mice. Cell **131:**1149–1163.
31. **Lee, J. H., et al.** 2010. Lysosomal proteolysis and autophagy require presenilin 1 and are disrupted by Alzheimer-related PS1 mutations. Cell **141:**1146–1158.
32. **Levine, B., and G. Kroemer.** 2008. Autophagy in the pathogenesis of disease. Cell **132:**27–42.
33. **Lindenbach, B. D., et al.** 2005. Complete replication of hepatitis C virus in cell culture. Science **309:**623–626.
34. **Lohmann, V., et al.** 1999. Replication of subgenomic hepatitis C virus RNAs in a hepatoma cell line. Science **285:**110–113.
35. **Manns, M. P., et al.** 2001. Peginterferon alfa-2b plus ribavirin compared with interferon alfa-2b plus ribavirin for initial treatment of chronic hepatitis C: a randomised trial. Lancet **358:**958–965.
36. **McHutchison, J. G., et al.** 2009. Telaprevir with peginterferon and ribavirin for chronic HCV genotype 1 infection. N. Engl. J. Med. **360:**1827–1838.
37. **Mizushima, N.** 2007. Autophagy: process and function. Genes Dev. **21:**2861–2873.
38. **Moradpour, D., F. Penin, and C. M. Rice.** 2007. Replication of hepatitis C virus. Nat. Rev. Microbiol. **5:**453–463.
39. **Moriishi, K., and Y. Matsuura.** 2007. Host factors involved in the replication of hepatitis C virus. Rev. Med. Virol. **17:**343–354.
40. **Moriishi, K., and Y. Matsuura.** 2003. Mechanisms of hepatitis C virus infection. Antivir. Chem. Chemother. **14:**285–297.
41. **Oda, K., Y. Nishimura, Y. Ikehara, and K. Kato.** 1991. Bafilomycin A1 inhibits the targeting of lysosomal acid hydrolases in cultured hepatocytes. Biochem. Biophys. Res. Commun. **178:**369–377.
42. **Orvedahl, A., et al.** 2007. HSV-1 ICP34.5 confers neurovirulence by targeting the Beclin 1 autophagy protein. Cell Host Microbe **1:**23–35.
43. **Poordad, F., et al.** 2011. Boceprevir for untreated chronic HCV genotype 1 infection. N. Engl. J. Med. **364:**1195–1206.
44. **Pua, H. H., I. Dzhagalov, M. Chuck, N. Mizushima, and Y. W. He.** 2007. A critical role for the autophagy gene Atg5 in T cell survival and proliferation. J. Exp. Med. **204:**25–31.
45. **Ramachandran, N., et al.** 2009. VMA21 deficiency causes an autophagic myopathy by compromising V-ATPase activity and lysosomal acidification. Cell **137:**235–246.
46. **Saito, K., et al.** 2008. Hepatitis C virus inhibits cell surface expression of HLA-DR, prevents dendritic cell maturation, and induces interleukin-10 production. J. Virol. **82:**3320–3328.
47. **Schmid, D., and C. Munz.** 2007. Innate and adaptive immunity through autophagy. Immunity **27:**11–21.
48. **Schutte, K., J. Bornschein, and P. Malfertheiner.** 2009. Hepatocellular carcinoma—epidemiological trends and risk factors. Dig. Dis. **27:**80–92.
49. **Sir, D., et al.** 2008. Induction of incomplete autophagic response by hepatitis C virus via the unfolded protein response. Hepatology **48:**1054–1061.
50. **Sloane, B. F., et al.** 2005. Cathepsin B and tumor proteolysis: contribution of the tumor microenvironment. Semin. Cancer Biol. **15:**149–157.
51. **Stankovic-Djordjevic, D., et al.** 2007. Hepatitis C virus genotypes and the development of hepatocellular carcinoma. J. Dig. Dis. **8:**42–47.
52. **Strader, D. B., T. Wright, D. L. Thomas, and L. B. Seeff.** 2004. Diagnosis, management, and treatment of hepatitis C. Hepatology **39:**1147–1171.
53. **Taguwa, S., et al.** 2009. Cochaperone activity of human butyrate-induced transcript 1 facilitates hepatitis C virus replication through an Hsp90-dependent pathway. J. Virol. **83:**10427–10436.
54. **Tal, M. C., et al.** 2009. Absence of autophagy results in reactive oxygen species-dependent amplification of RLR signaling. Proc. Natl. Acad. Sci. U. S. A. **106:**2770–2775.
55. **Tardif, K. D., and A. Siddiqui.** 2003. Cell surface expression of major histocompatibility complex class I molecules is reduced in hepatitis C virus subgenomic replicon-expressing cells. J. Virol. **77:**11644–11650.
56. **Wakita, T., et al.** 2005. Production of infectious hepatitis C virus in tissue culture from a cloned viral genome. Nat. Med. **11:**791–796.
57. **Walker, C. M.** 1997. Comparative features of hepatitis C virus infection in humans and chimpanzees. Springer Semin. Immunopathol. **19:**85–98.
58. **Wasley, A., and M. J. Alter.** 2000. Epidemiology of hepatitis C: geographic differences and temporal trends. Semin. Liver Dis. **20:**1–16.
59. **Wong, J., et al.** 2008. Autophagosome supports coxsackievirus B3 replication in host cells. J. Virol. **82:**9143–9153.
60. **Yoshimori, T., and T. Noda.** 2008. Toward unraveling membrane biogenesis in mammalian autophagy. Curr. Opin. Cell Biol. **20:**401–407.

JOURNAL OF VIROLOGY, Nov. 2011, p. 10976–10988 Vol. 85, No. 21
0022-538X/11/$12.00 doi:10.1128/JVI.00846-11

Heterogeneous Nuclear Ribonucleoprotein A2 Participates in the Replication of Japanese Encephalitis Virus through an Interaction with Viral Proteins and RNA▽

Hiroshi Katoh,[1] Yoshio Mori,[3] Hiroto Kambara,[1] Takayuki Abe,[1] Takasuke Fukuhara,[1] Eiji Morita,[1] Kohji Moriishi,[4] Wataru Kamitani,[2] and Yoshiharu Matsuura[1]*

Department of Molecular Virology[1] and Global COE Program,[2] Research Institute for Microbial Diseases, Osaka University, Osaka, Department of Virology III, National Institute of Infectious Diseases, Tokyo,[3] and Department of Microbiology, Faculty of Medicine, Yamanashi University, Yamanashi,[4] Japan

Received 26 April 2011/Accepted 9 August 2011

Japanese encephalitis virus (JEV) is a mosquito-borne flavivirus that is kept in a zoonotic transmission cycle between pigs and mosquitoes. JEV causes infection of the central nervous system with a high mortality rate in dead-end hosts, including humans. Many studies have suggested that the flavivirus core protein is not only a component of nucleocapsids but also an important pathogenic determinant. In this study, we identified heterogeneous nuclear ribonucleoprotein A2 (hnRNP A2) as a binding partner of the JEV core protein by pulldown purification and mass spectrometry. Reciprocal coimmunoprecipitation analyses in transfected and infected cells confirmed a specific interaction between the JEV core protein and hnRNP A2. Expression of the JEV core protein induced cytoplasmic retention of hnRNP A2 in JEV subgenomic replicon cells. Small interfering RNA (siRNA)-mediated knockdown of hnRNP A2 resulted in a 90% reduction of viral RNA replication in cells infected with JEV, and the reduction was cancelled by the expression of an siRNA-resistant hnRNP A2 mutant. In addition to the core protein, hnRNP A2 also associated with JEV nonstructural protein 5, which has both methyltransferase and RNA-dependent RNA polymerase activities, and with the 5′-untranslated region of the negative-sense JEV RNA. During one-step growth, synthesis of both positive- and negative-strand JEV RNAs was delayed by the knockdown of hnRNP A2. These results suggest that hnRNP A2 plays an important role in the replication of JEV RNA through the interaction with viral proteins and RNA.

Japanese encephalitis virus (JEV) belongs to the genus *Flavivirus* within the family *Flaviviridae*. Members of the genus *Flavivirus* are predominantly arthropod-borne viruses, such as dengue virus (DEN), West Nile virus (WNV), yellow fever virus (YFV), and tick-borne encephalitis virus, and frequently cause significant morbidity and mortality in mammals and birds (46). JEV is distributed in the south and southeast regions of Asia and is kept in a zoonotic transmission cycle between pigs or birds and mosquitoes (46, 69). JEV spreads to dead-end hosts, including humans, through the bite of JEV-infected mosquitoes and causes infection of the central nervous system, with a high mortality rate (46). JEV has a single-stranded positive-strand RNA genome of approximately 11 kb, which is capped at the 5′ end but lacks modification of the 3′ terminus by polyadenylation (38). The genomic RNA carries a single large open reading frame, and a polyprotein translated from the genome is cleaved co- and posttranslationally by host and viral proteases to yield three structural proteins—the core, precursor membrane, and envelope protein—and seven nonstructural (NS) proteins—NS1, NS2A, NS2B, NS3, NS4A, NS4B, and NS5 (61).

The core protein of flaviviruses has RNA-binding activity through basic amino acid clusters located in both the amino and carboxyl termini, indicating that the core protein forms a nucleocapsid interacting with viral RNA (23). In spite of the replication of flaviviruses in the cytoplasm, the core protein is also detected in the nucleus, especially the nucleolus, suggesting that the core protein plays an additional role in the life cycle of flaviviruses (6, 42, 48, 66). We previously reported that a mutant JEV defective in the nuclear localization of the core protein had impaired growth in mammalian cells and impaired neuroinvasiveness in mice (48) and that the nuclear and cytoplasmic localization of the JEV core protein is dependent on binding to the host nucleolar protein B23 (62). In addition to the JEV core protein, other flavivirus core proteins bind to several host proteins, such as Jab (a component of the COP9 signalosome complex) (53), the chaperone protein Hsp70 (54), heterogeneous nuclear ribonucleoprotein (hnRNP) K (7), and the apoptotic proteins HDM2 (71) and Daxx (50), and regulate their functions. In the cytoplasm, the core protein of flaviviruses was found at the sites of viral RNA replication (40, 68). A recent report demonstrated a coupling between viral RNA synthesis and RNA encapsidation (21, 55, 61). Therefore, the flavivirus core protein plays crucial roles not only in the viral life cycle, including RNA replication and assembly, but also in viral pathogenesis.

Replication of flaviviruses is initiated by a viral RNA replication complex through a process of RNA-dependent RNA polymerization on the endoplasmic reticulum (ER) membranes. The intracellular membrane rearrangements that are induced by the *Flaviviridae* family are best characterized for Kunjin virus (KUN), which is the Australian variant of WNV

* Corresponding author. Mailing address: Department of Molecular Virology, Research Institute for Microbial Diseases, Osaka University, 3-1 Yamada-oka, Suita, Osaka 565-0871, Japan. Phone: 81-6-6879-8340. Fax: 81-6-6879-8269. E-mail: matsuura@biken.osaka-u.ac.jp.

▽ Published ahead of print on 24 August 2011.

(14). KUN induces two distinct membrane structures: large clusters of double-membrane vesicles (DMV) and a second membrane structure that consists of convoluted membranes (CM). It has been demonstrated that DMV are the sites of viral replication, whereas CM are the sites of viral polyprotein processing (67). Clusters of DMV have also been observed in other flaviviruses (65). The NS3 and NS5 proteins have been identified as the major components of the viral RNA replication complex (4). NS5, the largest and most conserved flavivirus protein, contains sequences homologous to those of methyltransferase (MTase) and RNA-dependent RNA polymerase (RdRp), which are responsible for methylation of the 5′ cap structure (9, 27) and for viral RNA replication (1, 12, 74), respectively. In addition, NS5 inhibits the interferon-stimulated Jak-Stat signaling pathway through the activation of protein tyrosine phosphatases during JEV infection (37).

In this study, we identified hnRNP A2 as a binding partner of the JEV core protein by pulldown purification and mass spectrometry. hnRNP A2 and B1, which are the most abundant of the approximately 20 major hnRNPs, are produced by alternative splicing from a single gene and differ from each other by only a 12-amino-acid insertion in the N-terminal region of A2 (28). hnRNP A2 participates in posttranscriptional regulation in both the nucleus and cytoplasm and also is involved in telomere biogenesis. hnRNP A2 was translocated from the nucleus to the cytoplasm upon infection with JEV and facilitated viral replication through interaction with the JEV core and NS5 proteins and with the 5′-untranslated region (UTR) of the negative-strand JEV RNA, suggesting an important role for hnRNP A2 in the life cycle of JEV.

MATERIALS AND METHODS

Cells. Vero (African green monkey kidney), 293T (human kidney), and Huh7 (human hepatocellular carcinoma) cells were maintained in Dulbecco's modified Eagle's minimal essential medium (DMEM) supplemented with 100 U/ml penicillin, 100 μg/ml streptomycin, nonessential amino acids (Sigma, St. Louis, MO), and 10% fetal bovine serum (FBS). JEV subgenomic replicon (SGR) cells were generated as described previously (18). Briefly, Huh7 and 293T cells were electroporated with *in vitro*-transcribed RNA from pJErepIRESpuro, and drug-resistant clones were selected by treatment with puromycin (Invivogen, San Diego, CA) at a final concentration of 1 μg/ml. The resulting replicon cells were designated JEV-SGR-Huh7 and JEV-SGR-293T cells, respectively. Cell viability was determined by using CellTiter-Glo (Promega, Madison, WI) according to the manufacturer's instructions.

Plasmids. Plasmids encoding hemagglutinin (HA)-, FLAG-, and MEF (consisting of a myc tag, the tobacco etch virus protease cleavage site, and a FLAG tag)-tagged JEV core (pCAGPM-Core-HA, pCAGPM-FLAG-Core, and pCAGPM-MEF-Core, respectively) were prepared as described previously (49, 62). Plasmids encoding HA-tagged JEV NS proteins (pCAGPM-HA-NS) were generated by previously described methods (18). The cDNA of human hnRNP A2 was amplified by PCR and cloned into pcDNA 3.1 containing a FLAG tag gene (pcDNA 3.1 N-FLAG) (62), pCAGPM containing an HA tag gene (pCAGPM N-HA) (48), and pGEX 4T-1 (GE Healthcare, Buckinghamshire, United Kingdom) for expression in bacteria as a glutathione *S*-transferase (GST) fusion protein. The resulting plasmids were designated pcDNA-FLAG-hnRNP A2, pCAGPM-HA-hnRNP A2, and pGEX-hnRNP A2, respectively. A series of deletion mutants of the core protein, NS5, and hnRNP A2 was synthesized by PCR-based mutagenesis using a KOD-Plus mutagenesis kit (Toyobo, Osaka, Japan). A silent mutant of HA-hnRNP A2 (siR) and a mutant of FLAG-tagged core with Gly^{42} and Pro^{43} replaced by Ala (FLAG-CoreM) were also generated by PCR-based mutagenesis. All plasmids were confirmed by sequencing with an ABI Prism 3130 genetic analyzer (Applied Biosystems, Tokyo, Japan).

Antibodies. Anti-JEV core rabbit polyclonal antibody (PAb) was prepared as described previously (48). Anti-JEV NS3 mouse monoclonal antibody (MAb) was prepared by using a recombinant protein spanning amino acids (aa) 171 to 619 of JEV NS3. Anti-JEV NS5 mouse MAb was generated with recombinant NS5 at Bio Matrix Research Inc. (Chiba, Japan). Anti-FLAG mouse MAb (M2), anti-hnRNP A2/B1 mouse MAb (DP3B3), anti-β-actin mouse MAb, and anti-FLAG rabbit PAb were purchased from Sigma. Anti-nucleoporin p62 mouse MAb and anti-GM130 mouse MAb were purchased from BD Biosciences (Franklin Lakes, NJ). Anti-JEV envelope protein mouse MAb (6B4A-10), anti-HA mouse MAb (HA11), anti-PA28α rabbit PAb, anti-calregulin rabbit PAb (H-170), and anti-HA rat MAb (3F10) were purchased from Chemicon (Temecula, CA), Covance (Richmond, CA), Affinity Bioreagents (Golden, CO), Santa Cruz (California, CA), and Roche (Mannheim, Germany), respectively.

MEF purification. pCAGPM-MEF-Core was transfected into 293T cells and subjected to MEF purification as described previously (17, 62). Proteins interacting with the JEV core protein were separated by 12.5% sodium dodecyl sulfate-polyacrylamide gel electrophoresis (SDS-PAGE) and visualized by silver staining. The stained bands were excised, digested in gels with Lys-C, and analyzed by direct nanoflow liquid chromatography-tandem mass spectrometry (LC-MS/MS) (17).

Transfection, immunoprecipitation, and immunoblotting. Plasmids were transfected into 293T cells by use of TransIT LT1 (Mirus, Madison, WI), and cells were harvested at 24 h posttransfection and subjected to immunoprecipitation and immunoblotting as described previously (15). The immunoprecipitates were boiled in loading buffer and subjected to 12.5% or 15% SDS-PAGE. The proteins were transferred to polyvinylidene difluoride membranes (Millipore, Bedford, MA) and incubated with the appropriate antibodies. The immune complexes were visualized with SuperSignal West Femto substrate (Thermo Scientific, Rockford, IL) and detected by use of an LAS-3000 image analyzer system (Fujifilm, Tokyo, Japan).

Immunofluorescence microscopy and subcellular fractionation. Vero cells infected with JEV at a multiplicity of infection (MOI) of 1.0 or JEV-SGR-Huh7 cells transfected with pCAGPM-FLAG-Core and/or pCAGPM-HA-hnRNP A2 were fixed with cold acetone, incubated with appropriate antibodies, and examined by use of a Fluoview FV1000 laser scanning confocal microscope (Olympus, Tokyo, Japan) at 24 h postinfection/posttransfection. The subcellular localization of the proteins was determined by fractionation using a nuclear/cytosol fractionation kit (Biovision, Mountain, CA) according to the manufacturer's instructions.

Gene silencing. The small interfering RNAs (siRNAs) si-A2#1 (5′-GGAUU AUUUAAUAACAUU-3′) and si-A2#2 (5′-GGAGAGUAGUUGAGCCAA A-3′) (47) were used for knockdown of endogenous hnRNA A2/B1. The negative control, siCONTROL nontargeting siRNA-2 (si-NC), which exhibits no downregulation of any human genes, was purchased from Dharmacon (Buckinghamshire, United Kingdom). JEV-SGR-293T and naïve 293T cells grown on 6-, 12-, and 24-well plates were transfected with 30, 12, and 6 nM siRNA, respectively, by use of Lipofectamine RNAiMax (Invitrogen, Carlsbad, CA).

Real-time PCR. Total RNA was prepared from cells by use of an RNeasy minikit (Qiagen, Tokyo, Japan), and first-strand cDNA was synthesized using a ReverTra Ace qPCR RT kit (Toyobo). The level of each cDNA was determined by using Platinum SYBR green qPCR SuperMix UDG (Invitrogen), and fluorescent signals were analyzed by use of an ABI Prism 7000 system (Applied Biosystems). Strand-specific reverse transcription (RT) was performed using the following primers: 5′-ATGAGGCTGCCACACCAGAT-3′ for positive-strand JEV RNA, 5′-TACTCCGACGGTGTGGTCTA-3′ for negative-strand JEV RNA, and an oligo(dT) primer for β-actin mRNA. The JEV NS5 and β-actin genes were amplified using the following primer pairs: 5′-GCCGGGTGGGAC ACTAGAAT-3′ and 5′-TGGACAGCGATGTTCGTGAA-5′ for NS5 and 5′-A CGGGGTCACCCACACTGTGC-3′ and 5′-CTAGAAGCATTTGCGGTGGA CGATG-3′ for β-actin. The value of JEV RNA was normalized to that of β-actin mRNA.

Virus titration. Virus infectivity was determined by an immunostaining focus assay with Vero cells and was expressed in focus-forming units (FFU). Briefly, viruses were serially diluted and inoculated onto monolayers of Vero cells. After 1 h of absorption, cells were washed with serum-free DMEM and cultured in DMEM containing 5% FBS and 1.25% methylcellulose 4000. At 48 h postinfection, cells were fixed with 4% paraformaldehyde and permeabilized with 0.5% Triton X-100, and infectious foci were stained with anti-JEV envelope protein mouse MAb (6B4A-10) and visualized with a Vectastain Elite ABC anti-mouse IgG kit with VIP substrate (Vector Laboratories, Burlingame, CA).

Immunoprecipitation–RT-PCR. Cells (1×10^6) transfected with pCAGPM-HA-hnRNP A2 were infected with JEV at an MOI of 1.0 and then incubated with 400 μl of RNA-protein binding buffer (10 mM HEPES [pH 7.3], 500 mM KCl, 1 mM EDTA, 2 mM $MgCl_2$, 0.1% NP-40, yeast tRNA [0.1 μg/μl], RNase inhibitor [1 U/ml] [Toyobo], and protease inhibitor cocktail [Complete; Roche]) for 10 min at 4°C at 24 h postinfection. After centrifugation at 16,000 × *g* at 4°C for 20 min, the supernatants were incubated with 20 μl of protein G-Sepharose

4B Fast Flow beads (GE Healthcare) and 1 μg of normal mouse IgG for 1 h at 4°C. After centrifugation, the supernatants were further incubated with 1 μg of anti-HA mouse MAb or normal mouse IgG for 2 h at 4°C, and 25 μl of protein G-Sepharose beads was added. After 1 h of incubation at 4°C, the beads were washed five times with RNA-protein binding buffer without yeast tRNA, and RNA was isolated by use of TRIzol reagent (Invitrogen). RT-PCR was carried out using random hexamers and PrimeScript II reverse transcriptase (Takara Bio, Shiga, Japan), followed by PCR with PrimeSTAR GXL DNA polymerase (Takara Bio) and primers (5′-TCTGTCACTAGACTGGAGCA-3′ and 5′-CCA GAAACATCACCAGAAGG-3′) targeted to a fragment consisting of nucleotides 2652 to 3589 in the JEV NS1 gene.

***In vitro* transcription.** cDNA fragments encoding either the positive or negative strand of the 5′ and 3′ UTRs of JEV under the control of the T7 promoter were amplified by PCR. RNA transcripts were synthesized using a MEGAscript T7 kit (Ambion, Austin, TX). Biotinylated RNA was synthesized by adding 20 pmol of biotinylated UTP (biotin-16-UTP; Roche) to a 20-μl MEGAscript transcription reaction mix. Synthesized RNAs were purified using phenol-chloroform extraction and isopropanol precipitation and were analyzed in a 2% agarose gel.

RNA pulldown assay. Cell lysates (200 μg) extracted from 293T cells expressing HA-hnRNP A2 were incubated for 15 min at 30°C with the biotinylated JEV UTR RNA (10 pmol) in RNA-protein binding buffer and further incubated for 10 min at room temperature after addition of 250 μl streptavidin-conjugated MagneSphere paramagnetic particles (Promega). The RNA-protein complexes were washed five times with RNA-protein binding buffer without yeast tRNA and then subjected to SDS-PAGE and immunoblotting after boiling in 25 μl 2× SDS-PAGE sample buffer.

Preparation of recombinant hnRNP A2 and GST pulldown assay. GST-fused hnRNP A2 was expressed in *Escherichia coli* BL21(DE3) cells transformed with pGEX-hnRNP A2. Bacteria grown to an optical density at 600 nm of 0.6 were induced with 0.1 mM isopropyl-β-D-thiogalactopyranoside, incubated for 4 h at 37°C with shaking, collected by centrifugation at 6,000 × *g* for 10 min, lysed in 10 ml lysis buffer (50 mM Tris-HCl, pH 7.4, 150 mM NaCl, 1 mM EDTA, 1% Triton X-100) by sonication on ice, and centrifuged at 10,000 × *g* for 20 min. The supernatant was mixed with 200 μl of glutathione-Sepharose 4B beads (GE Healthcare) equilibrated with lysis buffer for 1 h at room temperature, and the beads were washed five times with lysis buffer and then replaced with RNA-protein binding buffer. Ten micrograms of GST or GST-hnRNP A2 was mixed with 10 pmol of the biotinylated positive or negative strand of the 3′ or 5′ UTR of JEV RNA for 15 min at 30°C with gentle agitation. The beads were washed five times with RNA-protein binding buffer without yeast tRNA.

Northern blotting. RNAs interacting with proteins were isolated by use of TRIzol reagent, separated by use of a formaldehyde-free RNA gel electrophoresis system (Amresco, Solon, OH), and transferred to a positively charged nylon membrane (Roche). The biotinylated RNA was detected with streptavidin conjugated with alkaline phosphatase (Roche) and visualized by chemiluminescence using CSPD (Roche).

RESULTS

Identification of hnRNP A2 as a binding partner of the JEV core protein. To identify cellular proteins associated with the JEV core protein, we employed an MEF affinity tag purification method. The MEF-Core protein was expressed in 293T cells and purified together with associated proteins as described previously (62). The silver-stained proteins were excised from an SDS-PAGE gel and analyzed by use of a nanoflow LC-MS/MS system. This procedure identified the amino acid sequences QEMQEVQSSR and GGGGNFGPGPGS NFR, which respond to amino acid residues 179 to 188 and 202 to 206 of human hnRNP A2, respectively. To confirm the interaction between the JEV core protein and hnRNP A2 in cells, 293T cells expressing FLAG-Core and HA-hnRNP A2 were examined by immunoprecipitation analyses. FLAG-Core and HA-hnRNP A2 were shown to be immunoprecipitated with each other (Fig. 1A). Furthermore, endogenous hnRNP A2 was coprecipitated with the JEV core protein in 293T cells infected with JEV but not in mock-infected cells (Fig. 1B). These results indicate that hnRNP A2 interacts with the JEV core protein.

Next, to determine the regions responsible for the interaction between JEV core and hnRNP A2, series of deletion mutants of the JEV core protein and hnRNP A2 were generated and examined by immunoprecipitation analyses. FLAG-Core (full length) and mutants lacking the N-terminal 20 and 40 amino acid residues (ΔN20 and ΔN40), but not those lacking the C-terminal 20 and 40 amino acid residues (ΔC65 and ΔC85), were immunoprecipitated with HA-hnRNP A2 (Fig. 1C). The flavivirus core protein has been shown to form homodimers via the central and C-terminal regions (26, 39). Therefore, to exclude the possibility that C-terminal deletion of the core protein abrogates dimerization, FLAG-Core (full length or ΔC85) and Core-HA (full length or ΔC85) were coexpressed and immunoprecipitated. As shown in Fig. 1D, the C-terminal deletion exhibited no effect on the homotypic interaction of the core protein, consistent with previous data showing that deletion of the C-terminal amino acid residues (aa 73 to 100) did not abolish the homotypic interaction of DEN core protein (64). These results indicate that the C-terminal region (aa 85 to 104) of the JEV core protein is responsible for the protein-protein interaction with hnRNP A2. hnRNP A2 is composed of two N-terminal RNA recognition motifs (RRM) followed by a Gly-rich C-terminal domain (GRD) (29). FLAG-hnRNP A2 (full length) and a mutant lacking the RRM1 domain (ΔRRM1), but not mutants lacking either RRM2 (ΔRRM2) or GRD (ΔGRD), were immunoprecipitated with Core-HA (Fig. 1E). The results indicated that the C-terminal residues from positions 85 to 104 of the JEV core protein and RRM2 and GRD in hnRNP A2 are responsible for the interaction.

hnRNP A2 translocates from the nucleus to the cytoplasm upon infection with JEV. To examine the intracellular localization of hnRNP A2 in cells infected with JEV, Vero cells expressing HA-hnRNP A2 were infected with JEV because an anti-hnRNP A2 antibody capable of detecting endogenous hnRNP A2 by immunofluorescence analysis was not available. We employed Vero cells, which exhibit a wider cytoplasm space than 293T cells, to investigate the cellular localization of each protein. Although HA-hnRNP A2 was detected mainly in the nucleus in mock-infected cells, as previously described (19), translocation of HA-hnRNP A2 into the nucleolus and cytoplasm and colocalization with the core protein were observed upon infection with JEV (Fig. 2A). HA-hnRNP A2 was detected in both the nucleus and cytoplasm in <60% of cells infected with JEV, while only 5% of mock-infected cells exhibited cytoplasmic localization of HA-hnRNP A2 (Fig. 2B). To further confirm the subcellular localization of hnRNP A2, the cytoplasmic and nuclear fractions of JEV-infected cells were analyzed by immunoblotting (Fig. 2C). hnRNP A2 was detected in both the cytoplasmic and nuclear fractions of the JEV-infected cells, while it was detected mainly in the nuclei of the mock-infected cells. These results indicate that infection of JEV induces translocation of hnRNP A2 from the nucleus to the cytoplasm.

Knockdown of hnRNP A2 decreases propagation of JEV. To determine the role of hnRNP A2 in the propagation of JEV, JEV was inoculated into 293T cells transfected with two siRNAs targeted to hnRNP A2/B1 (si-A2#1 and -2) or with a

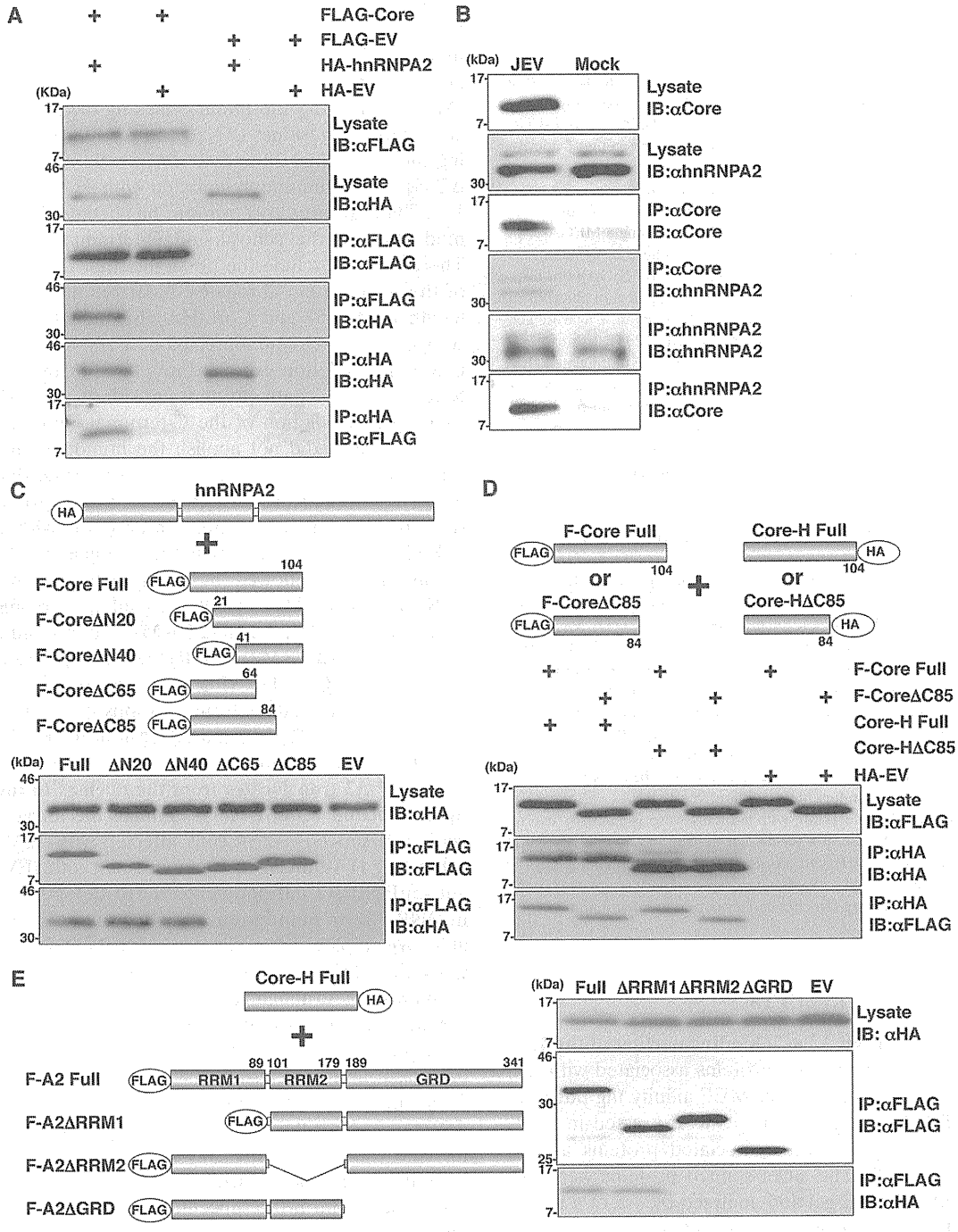

FIG. 1. Interaction of JEV core protein with hnRNP A2. (A) FLAG-Core and HA-hnRNP A2 were coexpressed in 293T cells and immunoprecipitated (IP) with mouse anti-HA MAb (HA11) or mouse anti-FLAG MAb (M2). The immunoprecipitates were subjected to immunoblotting (IB) to detect coprecipitated counterparts. As a negative control, an empty vector (EV) was used. (B) Interaction of JEV core protein with endogenous hnRNP A2 in 293T cells infected with JEV. Cells infected with JEV at an MOI of 1.0 were lysed at 24 h postinfection, and JEV core protein or hnRNP A2 was immunoprecipitated with rabbit anti-core PAb or mouse anti-hnRNP A2 MAb (DP3B3). The precipitates were analyzed by IB with appropriate antibodies. (C) Interaction of hnRNP A2 with deletion mutants of the JEV core protein. HA-hnRNP A2 and a series of deletion mutants of FLAG-Core were cotransfected in 293T cells, precipitated with mouse anti-FLAG MAb (M2), and then subjected to IB. (D) Dimerization of C-terminal deletion mutants of JEV core protein. FLAG-Core (full or ΔC85) and Core-HA (full or ΔC85) were cotransfected into 293T cells, treated with RNase A (10 μg/ml) for 30 min at 4°C, precipitated with mouse anti-HA MAb (HA11), and then subjected to IB. (E) Interaction of JEV core protein with deletion mutants of hnRNP A2. Core-HA and a series of deletion mutants of FLAG-hnRNP A2 were cotransfected into 293T cells and processed as described for panel C.

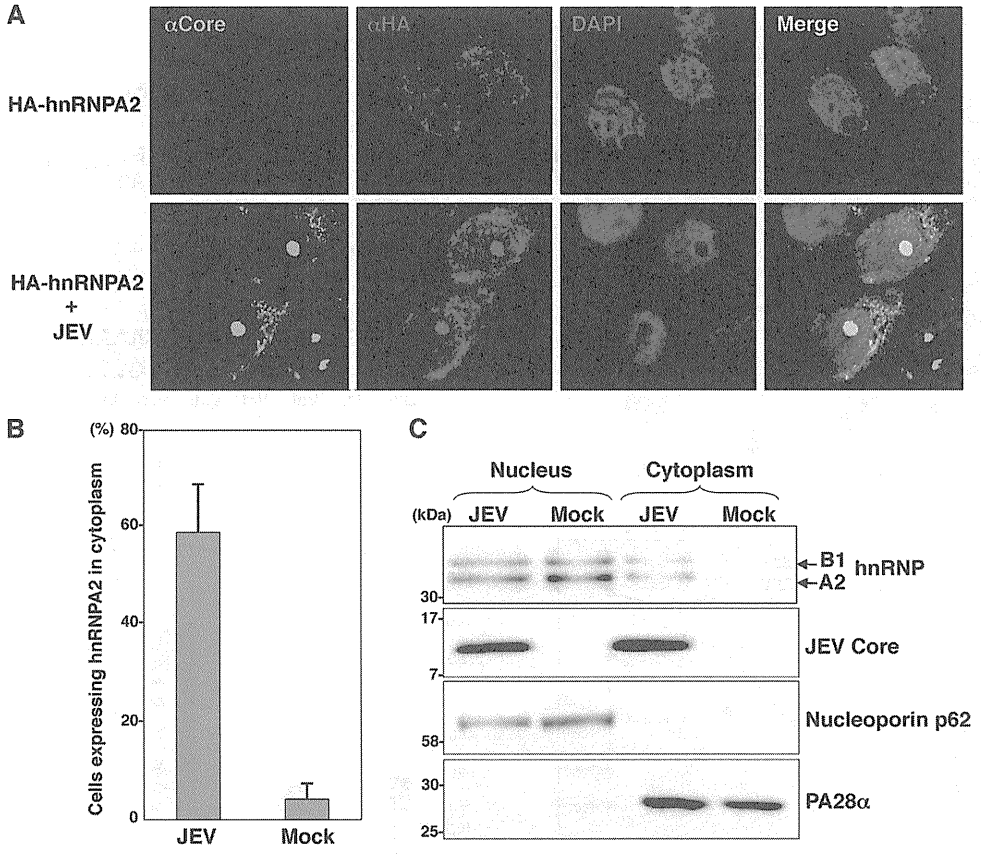

FIG. 2. Translocation of hnRNP A2 from the nucleus to the cytoplasm upon infection with JEV. (A) Vero cells transfected with a plasmid encoding HA-hnRNP A2 were infected with JEV at an MOI of 1.0 and then fixed with cold acetone at 24 h postinfection. JEV core and HA-hnRNP A2 were stained with rabbit anti-core PAb and mouse anti-HA MAb (HA11), followed by AF488-conjugated anti-rabbit IgG and AF594-conjugated anti-mouse IgG antibodies, respectively. Cell nuclei were stained with DAPI (4′,6-diamidino-2-phenylindole) (blue). (B) Percentages of cells exhibiting translocation of HA-hnRNP A2 to the cytoplasm. Three hundred cells expressing HA-hnRNP A2 were counted in three independent experiments. Error bars indicate the standard deviations of the means. (C) Intracellular fractionation of 293T cells infected with JEV. JEV core and hnRNP A2 in the nuclear and cytoplasmic fractions were detected by immunoblotting with rabbit anti-core PAb and mouse anti-hnRNP A2 MAb (DP3B3), respectively. Nucleoporin p62 and PA28α were used as nuclear and cytoplasmic markers, respectively.

control siRNA (si-NC) at 24 h posttransfection. Transfection of the siRNAs exhibited no cytotoxicity, so total RNA was extracted from the infected cells, and the level of JEV RNA was determined by real-time PCR at 24 h postinfection (Fig. 3A). The levels of JEV RNAs in cells transfected with si-A2#1 and -2 were reduced by approximately 40% and 90%, respectively, compared with those in cells treated with si-NC. The expression of JEV NS3 protein was decreased in accord with the reduction of hnRNP A2 (Fig. 3B). Furthermore, a reduction of viral production in the culture supernatants was observed by the knockdown of hnRNP A2 (Fig. 3C). To confirm the specificity of the suppression of JEV propagation by the knockdown of hnRNP A2, a mutant HA-hnRNP A2 protein resistant to si-A2#2 by the introduction of silent mutations (siR) was introduced into cells transfected with si-A2#2 (Fig. 3D). The reduction of JEV RNA propagation by the knockdown of hnRNP A2 was partially rescued by the expression of siR. These results suggest that hnRNP A2 is required for the propagation of JEV.

Translocation of hnRNP A2 from the nucleus to the ER by expression of JEV core protein enhances viral replication. Next, to determine the biological significance of hnRNP A2 in the replication of JEV RNA, we examined the effect of knockdown of hnRNP A2 in JEV-SGR-293T cells, since the subgenomic replicon RNA of JEV replicates autonomously in 293T cells in the absence of structural proteins. Knockdown of hnRNP A2 in the JEV-SGR-293T cells had no significant effect on the replication of the subgenomic RNA and the expression of the NS3 protein (Fig. 4A), suggesting that hnRNP A2 requires JEV structural proteins, probably the core protein, to enhance viral replication. To assess this possibility, we examined the effect of the exogenous expression of the JEV core protein on the subcellular localization of hnRNP A2 and the replication of the subgenomic RNA. HA-hnRNP A2 and FLAG-Core were coexpressed in subgenomic replicon Huh7 cells (JEV-SGR-Huh7) because these replicon cells were established in our laboratory previously (18). Huh7 cells exhibit a wider cytoplasmic view than 293T cells but have smaller and fewer nucleoli than Vero cells. HA-hnRNP A2 was detected in the nuclei of the Huh7 replicon cells transfected with an empty plasmid (Fig. 4B). Although FLAG-Core was not colocalized with calregulin, GM130, and EEA1, which are markers of the ER, Golgi apparatus, and early endosome, respectively, HA-hnRNP A2 was colocalized with FLAG-Core

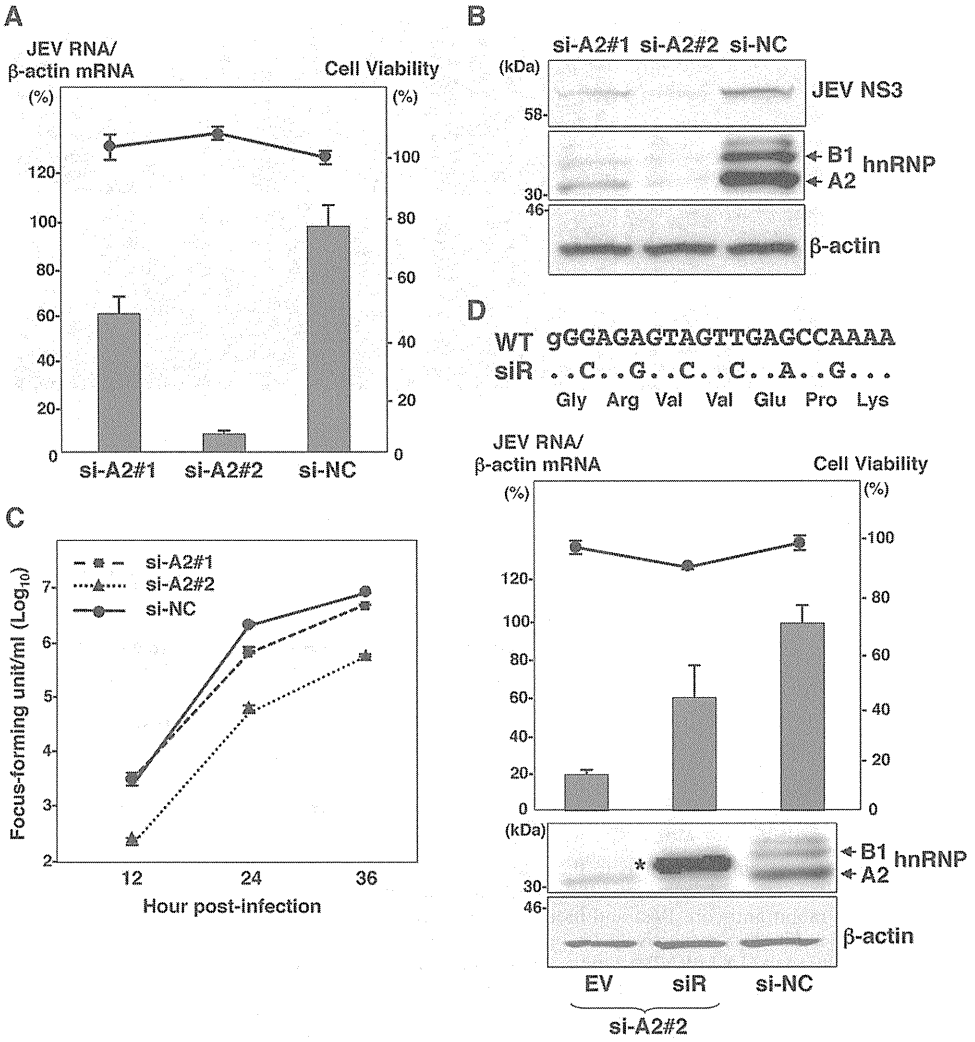

FIG. 3. Effect of hnRNP A2 knockdown on JEV propagation. (A) JEV was infected with 293T cells at an MOI of 1.0 24 h after transfection with si-A2#1, si-A2#2, or si-NC. Total cellular RNA was extracted at 24 h postinfection and subjected to RT. The level of JEV RNA (NS5) was determined by real-time PCR and calculated as a percentage of the control β-actin mRNA level (bar graph). Cell viability was determined 48 h after transfection with each siRNA and calculated as a percentage of the viability of cells treated with si-NC (line graph). The data are representative of three independent experiments. Error bars indicate the standard deviations of the means. (B) Cell lysates collected at 24 h postinfection were subjected to immunoblotting with mouse MAbs to JEV NS3, hnRNP A2 (DP3B3), and β-actin. (C) Culture supernatants were harvested at 12, 24, and 36 h postinfection, and infectious titers were determined by focus-forming assays in Vero cells. Closed squares, triangles, and circles indicate the infectious titers in the culture supernatants of cells transfected with si-A2#1, si-A2#2, and si-NC, respectively. The results shown are from three independent assays, with the error bars representing the standard deviations. (D) (Top) Nucleotide and amino acid sequences of wild-type (WT) and siRNA-resistant (siR) HA-hnRNP A2. Capital letters in the WT sequence indicate the target sequence of si-A2#2, and dots indicate the same nucleotides. (Middle) 293T cells cotransfected with si-A2#2 and siR or empty vector (EV) or transfected with si-NC were infected with JEV at an MOI of 1.0 at 24 h posttransfection. Total cellular RNA was extracted at 24 h postinfection and subjected to RT. The level of JEV RNA (NS5) was determined by real-time PCR and calculated as a percentage of the control β-actin mRNA level (bar graph). Cell viability was determined 48 h after transfection with each siRNA and calculated as a percentage of the viability of cells treated with si-NC (line graph). (Bottom) Cell lysates collected at 24 h postinfection were subjected to immunoblotting with hnRNP A2 (DP3B3) and β-actin. The exogenous mutant hnRNP A2 (siR) resistant to si-A2#2 is indicated by an asterisk. The data are representative of three independent experiments. Error bars indicate the standard deviations of the means.

and calregulin, but not with GM130 and EEA1, at 24 h posttransfection (Fig. 4B and data not shown). We have shown previously that two amino acid residues (Gly^{42} and Pro^{43}) in the JEV core protein are responsible for nuclear localization (47). To further confirm whether the cytoplasmic localization of hnRNP A2 by the expression of JEV core protein is caused by active export from the nucleus or passive retention in the cytoplasm, FLAG-CoreM, which is defective in nuclear localization, was introduced into JEV-SGR-Huh7 cells. As shown in Fig. 4B, hnRNP A2 was also detected in the ER of the replicon cells transfected with FLAG-CoreM. We further examined the interaction of hnRNP A2 with the core protein by an immunoprecipitation analysis. Coprecipitation of hnRNP A2 with core protein, but not with calregulin, was observed in the JEV-infected 293T cells (Fig. 4C). Next, to confirm the role of the core protein in the replication of JEV, FLAG-Core was

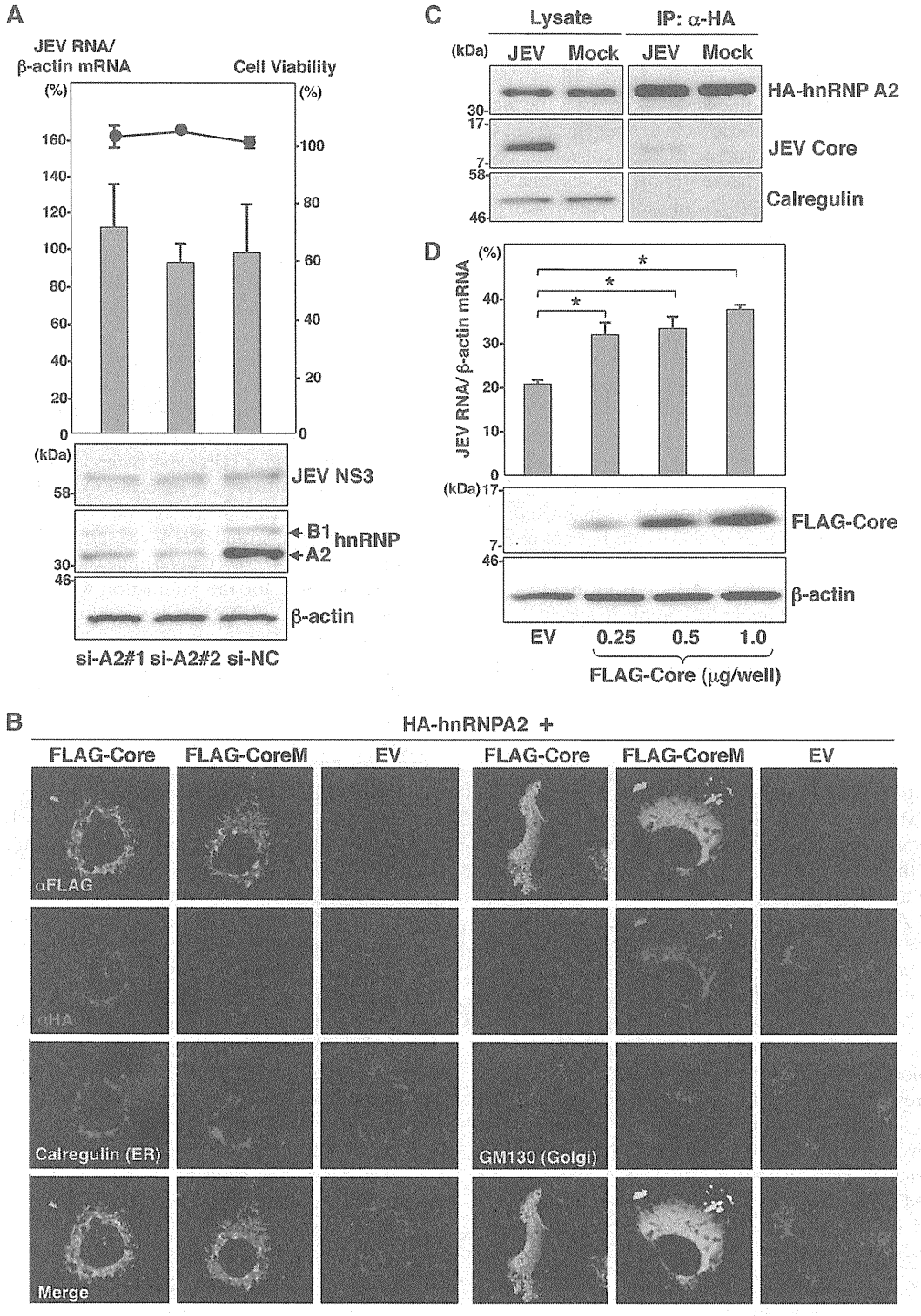

FIG. 4. Translocation of hnRNP A2 from the nucleus to the ER by expression of JEV core protein enhances viral RNA replication. (A) JEV subgenomic replicon (JEV-SGR-293T) cells were transfected with either si-A2#1, si-A2#2, or si-NC and harvested at 48 h posttransfection. (Top) The level of JEV RNA (NS5) was determined by real-time PCR and calculated as a percentage of the control β-actin mRNA level (bar graph). Cell viability was determined 48 h after transfection with each siRNA and was calculated as a percentage of the viability of cells treated with si-NC (line graph). (Bottom) Cell lysates collected at 48 h posttransfection were subjected to immunoblotting with mouse MAbs to JEV NS3, hnRNP A2 (DP3B3), and β-actin. (B) JEV subgenomic replicon (JEV-SGR-Huh7) cells were transfected with an expression plasmid for HA-hnRNP A2 together with that for FLAG-Core or FLAG-CoreM (a mutant defective in nuclear localization) or with an empty vector (EV) and then fixed with cold acetone at 24 h posttransfection. FLAG-Core was stained with either mouse anti-FLAG MAb (M2) and AF488-conjugated anti-mouse IgG or rabbit anti-FLAG PAb and AF488-conjugated anti-rabbit IgG. HA-hnRNP A2, calregulin, and GM130 were stained with rat anti-HA MAb (3F10), rabbit anti-calregulin PAb, and mouse anti-GM130 MAb, followed by AF594-conjugated anti-rat IgG, AF633-conjugated anti-rabbit IgG,

expressed in JEV-SGR-293T cells. As shown in Fig. 4D, the levels of JEV RNA were increased up to <2-fold, in accord with the expression levels of the core protein. The effect of JEV core expression on RNA replication in the subgenomic replicon cells was weak compared with that in the JEV-infected cells with hnRNP A2 knockdown (Fig. 3A); the weak effect might be attributable to the low efficiency of access of the exogenously expressed core protein to the replication complexes in the replicon cells. These results suggest that the passive ER retention of hnRNP A2 by interaction with the JEV core protein enhances viral replication.

hnRNP A2 interacts with JEV NS5 through interaction with viral RNA, in contrast to protein-protein interaction with JEV core protein. The viral RNA replication of flaviviruses takes place in a replication complex consisting of NS proteins and host proteins in the ER (45). To determine the interaction of hnRNP A2 with JEV NS proteins, FLAG-hnRNP A2 was coexpressed with each of the HA-tagged JEV NS proteins in JEV-SGR-293T cells and immunoprecipitated with anti-FLAG antibody. Among the JEV NS proteins we examined, only NS5 was coimmunoprecipitated with hnRNP A2 (Fig. 5A). More importantly, the interaction between hnRNP A2 and NS5 was observed in JEV-SGR-293T cells but not in 293T cells expressing both of the proteins (data not shown). Like the core protein, both NS5 and hnRNP A2 are RNA-binding proteins (23, 59, 74), and thus it might be feasible to speculate that viral RNA mediated the interplay between these proteins. To determine the role of viral RNA in these interactions, HA-hnRNP A2 and FLAG-Core were coexpressed in JEV-SGR-293T cells, and the cell lysates were treated with RNase A before immunoprecipitation (Fig. 5B). Coprecipitation of NS5 with hnRNP A2 in the replicon cells was abolished by the treatment with RNase A, while that of JEV core protein with hnRNP A2 was rather resistant to the treatment. The RNA-mediated interaction between NS5 and hnRNP A2 was also observed in the JEV-infected cells, but not that between the core protein and hnRNP A2 (Fig. 5C). These results indicate that hnRNP A2 interacts with JEV NS5 through the interaction with viral RNA, in contrast to protein-protein interaction with the JEV core protein. Next, to determine the subcellular localization of NS5 and hnRNP A2, Vero cells expressing HA-hnRNP A2 were infected with JEV and examined by confocal microscopy at 24 h postinfection. Both hnRNP A2 and NS5 were colocalized in the ER of cells infected with JEV (Fig. 5D). These results suggest that hnRNP A2 interacts with JEV core protein and NS5A around the ER (Fig. 4B) and in the ER, respectively. To determine the region in NS5 responsible for the interaction with hnRNP A2, three HA-NS5 mutants, lacking the MTase region (ΔMET), the internal linker region (ΔILR), and the RdRp region (ΔRdRp), were coexpressed with FLAG-hnRNP A2 in JEV-SGR-293T cells. FLAG-hnRNP A2 was immunoprecipitated with each of the NS5 constructs except for the mutant lacking the MTase region (Fig. 5E). On the other hand, NS5 was coprecipitated with full-length hnRNP A2 (FLAG-A2 Full) and with a mutant lacking the RRM1 domain (FLAG-A2 ΔRRM1) but not with mutants lacking either RRM2 or GRD (FLAG-A2 ΔRRM2 or FLAG-A2 ΔGRD) (Fig. 5F). These results indicate that RRM2 and GRD in hnRNP A2 participate in the interaction with the MTase region in NS5 as well as with the C-terminal region of the JEV core protein, as described above (Fig. 1E).

hnRNP A2 interacts with the 5′ UTR of the negative-sense JEV RNA and facilitates viral RNA synthesis. Next, to determine the interaction between hnRNP A2 and JEV RNA, 293T cells expressing HA-hnRNP A2 were inoculated with JEV, and the cell lysates were immunoprecipitated with an anti-HA antibody at 24 h postinfection. RNAs extracted from the precipitates were subjected to RT-PCR to detect JEV RNA. JEV NS1 RNA was detected in the precipitates obtained by anti-HA antibody for cells expressing HA-hnRNP A2 (Fig. 6A), suggesting that hnRNP A2 associates with JEV RNA. Several hnRNPs have been shown to interact with the UTR of the viral RNA of positive-strand RNA viruses, such as poliovirus and enterovirus 71 (5, 35). To determine the region in the UTRs of JEV responsible for the interaction with hnRNP A2, biotin-labeled 5′ and 3′ UTRs of the positive- and negative-sense JEV RNAs were synthesized *in vitro* (Fig. 6B), and a pulldown assay was carried out using streptavidin beads to capture the biotinylated viral RNA associated with HA-hnRNP A2 in 293T cells. HA-hnRNP A2 was pulled down with the 5′ UTR of the negative-strand viral RNA but not with other viral RNAs. To further confirm the interaction between hnRNP A2 and the viral RNA, GST-hnRNP A2 prepared in *E. coli* was incubated with the biotinylated 5′ UTR of the negative-strand JEV RNA or 3′ UTR of the positive-strand JEV RNA, and the viral RNA interacting with GST-hnRNP A2 was detected by Northern blot analyses using streptavidin. The 5′ UTR of the negative-strand JEV RNA was detected in the complex (Fig. 6C). These results indicate that hnRNP A2 interacts directly with the 5′ UTR of the negative-strand JEV RNA.

As described for Fig. 3, knockdown of hnRNP A2 suppresses JEV propagation. To further examine the roles of hnRNP A2 in viral RNA replication in more detail, syntheses of the positive- and negative-strand viral RNAs were determined for cells transfected with si-A2#2 targeted to hnRNP A2 and inoculated with JEV at 24 h posttransfection. Total RNAs extracted from the infected cells at various time points were reverse transcribed by using strand-specific primers for either the 5′ UTR of the negative-strand JEV RNA or the 3′ UTR of the positive-strand JEV RNA, with oligo(dT) primers used for

and AF633-conjugated anti-mouse IgG antibodies, respectively. (C) HA-hnRNP A2 was expressed in 293T cells, which were infected with JEV at an MOI of 1.0 and subjected to immunoprecipitation with mouse anti-HA MAb (HA11) at 24 h postinfection. The immunoprecipitates were subjected to immunoblotting using rat anti-HA MAb (3F10), rabbit anti-core PAb, or rabbit anti-calregulin PAb. (D) JEV-SGR-293T cells were transfected with empty vector (EV) or a plasmid encoding FLAG-Core, and the level of JEV RNA (NS5) was determined by real-time PCR at 48 h posttransfection and calculated as a percentage of the control β-actin mRNA level. The data are representative of three independent experiments. Error bars indicate the standard deviations of the means. The significance of differences between the means was determined by Student's *t* test.

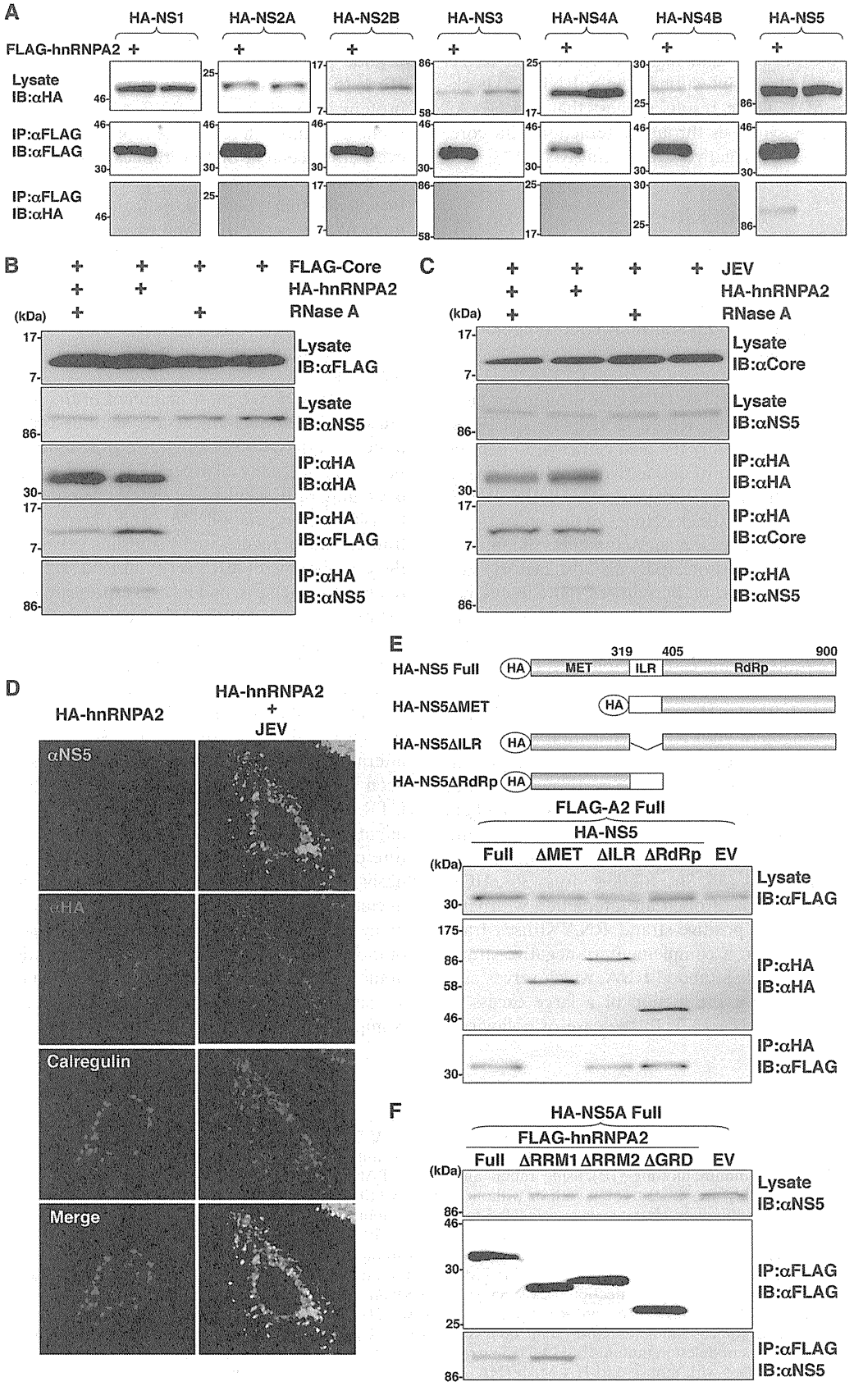
A
HA-NS1
HA-NS2A
HA-NS2B
HA-NS3
HA-NS4A
HA-NS4B
HA-NS5
FLAG-hnRNPA2
Lysate IB:αHA
IP:αFLAG IB:αFLAG
IP:αFLAG IB:αHA
B
FLAG-Core
HA-hnRNPA2
RNase A
(kDa)
Lysate IB:αFLAG
Lysate IB:αNS5
IP:αHA IB:αHA
IP:αHA IB:αFLAG
IP:αHA IB:αNS5
C
JEV
HA-hnRNPA2
RNase A
(kDa)
Lysate IB:αCore
Lysate IB:αNS5
IP:αHA IB:αHA
IP:αHA IB:αCore
IP:αHA IB:αNS5
D
HA-hnRNPA2
HA-hnRNPA2 + JEV
αNS5
αHA
Calregulin
Merge
E
HA-NS5 Full
HA-NS5ΔMET
HA-NS5ΔILR
HA-NS5ΔRdRp
HA
MET
ILR
RdRp
319
405
900
FLAG-A2 Full
HA-NS5
Full ΔMET ΔILR ΔRdRp EV
(kDa)
Lysate IB:αFLAG
IP:αHA IB:αHA
IP:αHA IB:αFLAG
F
HA-NS5A Full
FLAG-hnRNPA2
Full ΔRRM1 ΔRRM2 ΔGRD EV
(kDa)
Lysate IB:αNS5
IP:αFLAG IB:αFLAG
IP:αFLAG IB:αNS5

β-actin mRNA as an internal control, and JEV RNA and β-actin mRNA levels were determined by real-time PCR. Syntheses of both the positive- and negative-strand viral RNAs were delayed from 12 h postinfection in the hnRNP A2 knockdown cells (Fig. 6D). These results suggest that hnRNP A2 facilitates viral RNA synthesis through interaction with core, NS5, and the 5′ UTR of negative-strand viral RNA.

DISCUSSION

The flavivirus core protein is a multifunctional protein involved in viral replication and pathogenesis. The core protein binds to the viral RNA and forms a nucleocapsid in the cytoplasm as a structural protein (23). Furthermore, some portion of the core protein of flaviviruses localizes in the nucleus and associates with various host factors, such as B23 (62), Hsp70 (54), Daxx (50), and Jab1 (53). The DEN core protein has been shown to interact with hnRNP K and to regulate C/EBP-β-mediated transcription to modify the host cell environment by regulating the expression of pro- and antiviral factors for viral propagation (7). In addition, the core proteins of DEN, WNV, and hepatitis C virus (HCV), which belongs to the genus *Hepacivirus* within the family *Flaviviridae*, have functions of inducing or inhibiting the apoptosis associated with host factors, suggesting that the core protein of flaviviruses participates not only in viral assembly (as a structural protein) but also in pathogenesis (as a nonstructural protein) (13, 34, 43, 58, 70). The flavivirus core protein is not essential for RNA replication, since NS proteins alone are sufficient for efficient replication of the subgenomic viral RNA (24), while the core protein has been suggested to augment viral RNA replication (48).

In this study, we demonstrated that the JEV core protein specifically interacts with hnRNP A2 and participates in viral replication. Many RNA-binding proteins, including members of the hnRNP complex, have been shown to participate in the life cycles of several positive-strand RNA viruses, such as poliovirus (5), enterovirus 71 (35, 36), Sindbis virus (36), HCV (25), and DEN (7, 20, 51), through an interaction with viral RNA. The RdRp of the positive-strand RNA viruses transcribes the viral RNA into a complementary negative-strand RNA and generates double-stranded RNA, which serves as a replicative intermediate for production of a large excess of positive-strand genomic RNA (32). In the case of poliovirus, hnRNP C1/C2 has been shown to be involved in the initiation of viral RNA synthesis through the interaction with viral replication polypeptides and the 3′ UTR of the negative-strand RNA (5). In this study, we have shown that the JEV core protein interacts with hnRNP A2 and participates in RNA replication through recruitment of hnRNP A2 to the ER; however, enhancement of JEV replication could not be explained by the interaction of the core protein with hnRNP A2. Therefore, we further examined the factors involved in the enhancement of JEV replication and found that hnRNP A2 also associates with NS5 and the 5′ UTR of negative-strand viral RNA. These findings suggest that hnRNP A2 participates in positive-strand RNA synthesis through the interaction with viral proteins and RNA. Further studies are needed to clarify the molecular mechanisms by which hnRNP A2 promotes viral RNA replication.

hnRNP A2 is the most abundant of the hnRNP family proteins and is the first *trans*-acting factor described to be involved in neural mRNA trafficking (59). In addition, hnRNP A2 participates in virtually all aspects of mRNA processing, including packaging of nascent transcripts, splicing of pre-mRNAs, and translational regulation (16), and plays crucial roles in post-transcriptional regulation by shuttling between the nucleus and the cytoplasm with mRNA (8). hnRNP A2 also participates in telomere biogenesis, and its overexpression has been described for many cancer cell lines derived from the breast, pancreas, liver, and gastrointestinal tract (30, 31, 72, 75). In virus infections, hnRNP A2 has been shown to enhance mouse hepatitis virus RNA synthesis (60) and to regulate the trafficking of genomic RNA of human immunodeficiency virus (33). Although in this study we have demonstrated that hnRNP A2 interacts with the 5′ UTR of negative-strand JEV RNA, it has been shown previously that hnRNP A2 interacts with the 3′ UTR of positive-strand DEN RNA (55). This discrepancy might be attributable to differences in sequence and/or structure of the UTRs between JEV and DEN, as reported previously (21). Localization of hnRNP A2 was changed from the nucleus to the cytoplasm upon infection with JEV, as seen in many other virus infections (5, 25, 35). In addition, expression of the JEV core protein alone induced retention of hnRNP A2 in the ER and facilitated RNA replication in the replicon cells, suggesting that interaction of the core protein with hnRNP A2 is important for RNA replication of JEV.

FIG. 5. hnRNP A2 forms a complex with JEV core protein and NS5 via JEV RNA. (A) FLAG-hnRNP A2 was coexpressed with HA-JEV NS proteins in JEV subgenomic replicon (JEV-SGR-293T) cells and immunoprecipitated (IP) with mouse anti-FLAG MAb (M2). The immunoprecipitates were subjected to immunoblotting (IB) using rabbit anti-FLAG PAb. (B) FLAG-Core and HA-hnRNP A2 were coexpressed in JEV-SGR-293T cells, and cell lysates were treated with or without RNase A (10 μg/ml) for 30 min at 4°C and immunoprecipitated with mouse anti-HA MAb (HA11). The immunoprecipitates were subjected to IB with rabbit anti-FLAG PAb, mouse anti-NS5 MAb, or rat anti-HA MAb (3F10). (C) HA-hnRNP A2 was expressed in 293T cells, which were infected with JEV at an MOI of 1.0 and subjected to IP with mouse anti-HA MAb (HA11) at 24 h postinfection. The cell lysates were pretreated with or without RNase A (10 μg/ml) for 30 min at 4°C. The immunoprecipitates were subjected to IB using rabbit anti-core PAb, mouse anti-NS5 MAb, or rat anti-HA MAb (3F10). (D) Vero cells infected with JEV at an MOI of 1.0 and fixed with cold acetone at 24 h postinfection. JEV NS5, HA-hnRNP A2, and calregulin, which is an ER marker, were stained with mouse anti-NS5 MAb, rat anti-HA MAb (3F10), and anti-calregulin rabbit PAb (H-170), followed by AF488-conjugated anti-mouse IgG, AF594-conjugated anti-rat IgG, and AF633-conjugated anti-rabbit IgG, respectively. (E) Interaction of hnRNP A2 with deletion mutants of JEV NS5. FLAG-hnRNP A2 and a series of deletion mutants of HA-NS5 were cotransfected into JEV-SGR-293T cells. Deletion mutants of HA-NS5 in cell lysates were immunoprecipitated with mouse anti-HA MAb (HA11), and the immunoprecipitates were subjected to IB with mouse anti-FLAG MAb (M2) or rat anti-HA MAb (3F10). (F) Interaction of JEV NS5 with deletion mutants of hnRNP A2. A series of deletion mutants of FLAG-hnRNP A2 were expressed in JEV-SGR-293T cells and were immunoprecipitated with mouse anti-FLAG MAb (M2). The immunoprecipitates were subjected to IB with rabbit anti-FLAG PAb or mouse anti-NS5 MAb.

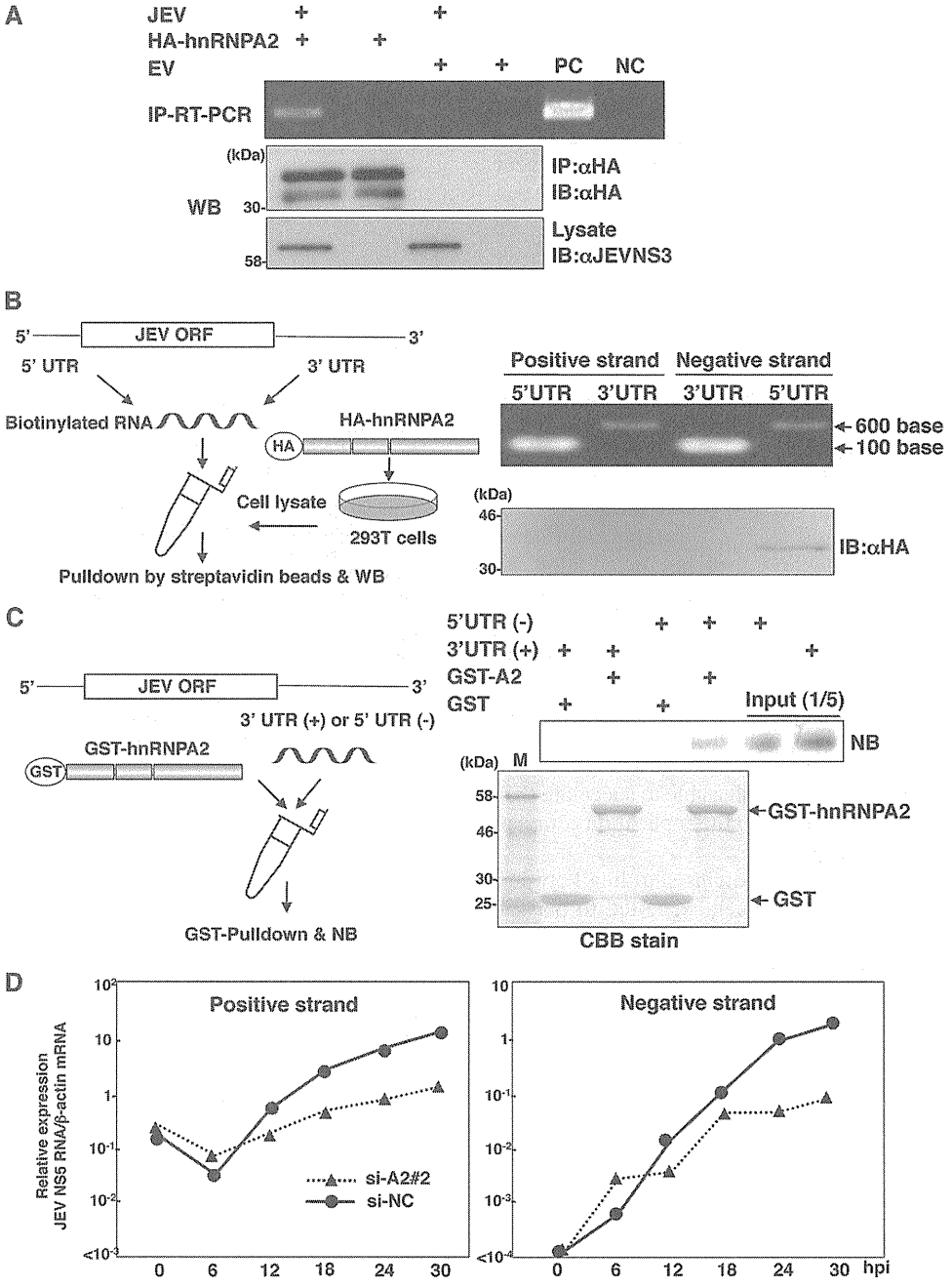

FIG. 6. hnRNP A2 interacts with the 5′ UTR of the negative-strand JEV RNA and facilitates viral RNA synthesis. (A) A plasmid encoding HA-hnRNP A2 was transfected into 293T cells, which were infected with JEV at an MOI of 1.0 at 24 h posttransfection. Cell lysates harvested at 24 h postinfection were immunoprecipitated with mouse anti-HA MAb (HA11) and subjected to IB with rat anti-HA MAb (3F10). RNAs extracted from the immunoprecipitates were subjected to RT. JEV RNA was detected by PCR using primers targeting the NS1 region. (B) Cell lysates from 293T cells transfected with a plasmid encoding HA-hnRNP A2, prepared at 24 h posttransfection, were incubated with the biotin-labeled 5′ or 3′ UTR of the positive- or negative-sense JEV RNA for 15 min at 30°C. After pulldown by streptavidin, protein complexes were subjected to IB with mouse anti-HA MAb (HA11). (C) GST-fused hnRNP A2 prepared in bacteria was incubated with the biotin-labeled 3′ UTR of positive-sense JEV RNA or 5′ UTR of negative-sense JEV RNA for 15 min at 30°C. RNAs extracted from the precipitates obtained by GST pulldown were subjected to Northern blotting (NB) with streptavidin. CBB, Coomassie brilliant blue. (D) Total RNA extracted from 293T cells transfected with si-A2#2 or si-NC and infected with JEV at an MOI of 10 at 24 h posttransfection was subjected to RT using strand-specific primers and an oligo(dT) primer. The levels of positive- and negative-strand JEV RNAs (NS5) were determined by real-time PCR and calculated as percentages of the control β-actin mRNA level. Closed triangles and circles indicate the relative RNA levels in cells transfected with si-A2#2 and si-NC, respectively. The data are representative of three independent experiments.

Although replication and packaging of the viral genome remain obscure steps in the life cycle of flaviviruses, coupling between RNA replication and particle assembly has been suggested to occur in several positive-strand RNA viruses (22, 52). Replication of flaviviruses takes place in virus-induced intracellular membrane structures on the ER known as replication complexes, which contain NS proteins, viral RNA, and host factors essential for replication, and is suggested to circumvent the activation of the host immune response triggered by viral RNA (45). The invagination of the ER membrane induced by the expression of NS proteins is connected to the cytoplasm through pores, which allows entry of nucleotides and other factors required for RNA replication and for exit of the newly synthesized RNA to the sites for translation and particle assembly (10, 44, 65). The majority of the viral RNA species in the replication complex exist as double-stranded replicative intermediates, and newly transcribed genomic RNA is exported efficiently from the replication complex to the assembly sites (10). In addition, to minimize the production of defective viral RNA transcribed from the error-prone viral RdRp (22), viral RNA must be synthesized from active replication complexes consisting of viral and host proteins; in addition, to circumvent the induction of innate immunity, the viral genome should be packaged immediately into viral particles. Therefore, structural and nonstructural viral proteins participate coordinately in viral RNA replication and particle formation, as reported for the participation of the NS3 protein of YFV in viral assembly (56). Although the biological significance of the interaction between the JEV core protein and hnRNP A2 for viral replication is unclear, it might be feasible to speculate that the core protein recruits hnRNP A2 to the replication complex to promote viral RNA replication.

The property of hnRNP family proteins shuttling between the cytoplasm and the nucleus has been suggested to participate in the maintenance of cellular homeostasis in response to stress stimuli such as heat shock (57), amino acid starvation (41), mitochondrial dysfunction (11), and nucleolar stresses (73). Infection of positive-strand RNA viruses modulates the host environment for efficient viral propagation through the remodeling of host proteins. For instance, the core protein of WNV suppresses the expression of the ER stress-protective protein OASIS and inhibits the antiviral response through induction of ER stress (2, 63), while poliovirus infection increases nuclear envelope permeability and replaces nuclear proteins required for efficient viral replication in the cytoplasm (3). In this study, hnRNP A2 was localized in both the nucleus and the cytoplasm upon infection with JEV or expression of the JEV core protein, suggesting that the JEV core protein plays an important role in the replication of JEV RNA through a modification of the host cellular environment.

Viruses are obligatory intracellular parasites, and therefore they are completely dependent on infected cells to supply energy, chemicals, and much of the machinery required for their replication. In the present study, we identified hnRNP A2 as one of the host factors participating in JEV propagation. The ER retention of hnRNP A2 through an interaction with the core protein leads to the interaction of hnRNP A2 with NS5 and the negative-strand viral RNA, resulting in the promotion of JEV RNA replication. This may help to open up a new area of inquiry into virus-cell interactions and could lead to an improved understanding of the mechanism of flavivirus RNA replication.

ACKNOWLEDGMENTS

We thank H. Murase and M. Tomiyama for their secretarial assistance. We also thank E. Konishi for providing a plasmid.

This work was supported in part by grants-in-aid from the Ministry of Health, Labor, and Welfare, the Ministry of Education, Culture, Sports, Science, and Technology, and the Osaka University Global Center of Excellence Program. H. Katoh is a research fellow of the Japanese Society for the Promotion of Science.

REFERENCES

1. **Ackermann, M., and R. Padmanabhan.** 2001. De novo synthesis of RNA by the dengue virus RNA-dependent RNA polymerase exhibits temperature dependence at the initiation but not elongation phase. J. Biol. Chem. **276:** 39926–39937.
2. **Ambrose, R. L., and J. M. Mackenzie.** 2011. West Nile virus differentially modulates the unfolded protein response to facilitate replication and immune evasion. J. Virol. **85:**2723–2732.
3. **Belov, G. A., et al.** 2000. Early alteration of nucleocytoplasmic traffic induced by some RNA viruses. Virology **275:**244–248.
4. **Bollati, M., et al.** 2010. Structure and functionality in flavivirus NS-proteins: perspectives for drug design. Antiviral Res. **87:**125–148.
5. **Brunner, J. E., et al.** 2005. Functional interaction of heterogeneous nuclear ribonucleoprotein C with poliovirus RNA synthesis initiation complexes. J. Virol. **79:**3254–3266.
6. **Bulich, R., and J. G. Aaskov.** 1992. Nuclear localization of dengue 2 virus core protein detected with monoclonal antibodies. J. Gen. Virol. **73:**2999–3003.
7. **Chang, C. J., et al.** 2001. The heterogeneous nuclear ribonucleoprotein K (hnRNP K) interacts with dengue virus core protein. DNA Cell Biol. **20:** 569–577.
8. **Dreyfuss, G., M. J. Matunis, S. Pinol-Roma, and C. G. Burd.** 1993. hnRNP proteins and the biogenesis of mRNA. Annu. Rev. Biochem. **62:**289–321.
9. **Egloff, M. P., D. Benarroch, B. Selisko, J. L. Romette, and B. Canard.** 2002. An RNA cap (nucleoside-2′-*O*-)-methyltransferase in the flavivirus RNA polymerase NS5: crystal structure and functional characterization. EMBO J. **21:**2757–2768.
10. **Gillespie, L. K., A. Hoenen, G. Morgan, and J. M. Mackenzie.** 2010. The endoplasmic reticulum provides the membrane platform for biogenesis of the flavivirus replication complex. J. Virol. **84:**10438–10447.
11. **Guha, M., W. Tang, N. Sondheimer, and N. G. Avadhani.** 2010. Role of calcineurin, hnRNPA2 and Akt in mitochondrial respiratory stress-mediated transcription activation of nuclear gene targets. Biochim. Biophys. Acta **1797:**1055–1065.
12. **Guyatt, K. J., E. G. Westaway, and A. A. Khromykh.** 2001. Expression and purification of enzymatically active recombinant RNA-dependent RNA polymerase (NS5) of the flavivirus Kunjin. J. Virol. Methods **92:**37–44.
13. **Hahn, C. S., Y. G. Cho, B. S. Kang, I. M. Lester, and Y. S. Hahn.** 2000. The HCV core protein acts as a positive regulator of Fas-mediated apoptosis in a human lymphoblastoid T cell line. Virology **276:**127–137.
14. **Hall, R. A., J. H. Scherret, and J. S. Mackenzie.** 2001. Kunjin virus: an Australian variant of West Nile? Ann. N. Y. Acad. Sci. **951:**153–160.
15. **Hamamoto, I., et al.** 2005. Human VAP-B is involved in hepatitis C virus replication through interaction with NS5A and NS5B. J. Virol. **79:**13473–13482.
16. **Han, S. P., et al.** 2010. Differential subcellular distributions and trafficking functions of hnRNP A2/B1 spliceoforms. Traffic **11:**886–898.
17. **Ichimura, T., et al.** 2005. 14-3-3 proteins modulate the expression of epithelial Na+ channels by phosphorylation-dependent interaction with Nedd4-2 ubiquitin ligase. J. Biol. Chem. **280:**13187–13194.
18. **Kambara, H., et al.** 2011. Involvement of cyclophilin B in the replication of Japanese encephalitis virus. Virology **412:**211–219.
19. **Kamma, H., et al.** 1999. Molecular characterization of the hnRNP A2/B1 proteins: tissue-specific expression and novel isoforms. Exp. Cell Res. **246:** 399–411.
20. **Kanlaya, R., S. N. Pattanakitsakul, S. Sinchaikul, S. T. Chen, and V. Thongboonkerd.** 2010. Vimentin interacts with heterogeneous nuclear ribonucleoproteins and dengue nonstructural protein 1 and is important for viral replication and release. Mol. Biosyst. **6:**795–806.
21. **Khromykh, A. A., H. Meka, K. J. Guyatt, and E. G. Westaway.** 2001. Essential role of cyclization sequences in flavivirus RNA replication. J. Virol. **75:**6719–6728.
22. **Khromykh, A. A., A. N. Varnavski, P. L. Sedlak, and E. G. Westaway.** 2001. Coupling between replication and packaging of flavivirus RNA: evidence derived from the use of DNA-based full-length cDNA clones of Kunjin virus. J. Virol. **75:**4633–4640.
23. **Khromykh, A. A., and E. G. Westaway.** 1996. RNA binding properties of core protein of the flavivirus Kunjin. Arch. Virol. **141:**685–699.

24. **Khromykh, A. A., and E. G. Westaway.** 1997. Subgenomic replicons of the flavivirus Kunjin: construction and applications. J. Virol. **71:**1497–1505.
25. **Kim, C. S., S. K. Seol, O. K. Song, J. H. Park, and S. K. Jang.** 2007. An RNA-binding protein, hnRNP A1, and a scaffold protein, septin 6, facilitate hepatitis C virus replication. J. Virol. **81:**3852–3865.
26. **Kofler, R. M., F. X. Heinz, and C. W. Mandl.** 2002. Capsid protein C of tick-borne encephalitis virus tolerates large internal deletions and is a favorable target for attenuation of virulence. J. Virol. **76:**3534–3543.
27. **Koonin, E. V.** 1993. Computer-assisted identification of a putative methyltransferase domain in NS5 protein of flaviviruses and lambda 2 protein of reovirus. J. Gen. Virol. **74:**733–740.
28. **Kozu, T., B. Henrich, and K. P. Schafer.** 1995. Structure and expression of the gene (HNRPA2B1) encoding the human hnRNP protein A2/B1. Genomics **25:**365–371.
29. **Landsberg, M. J., K. Moran-Jones, and R. Smith.** 2006. Molecular recognition of an RNA trafficking element by heterogeneous nuclear ribonucleoprotein A2. Biochemistry **45:**3943–3951.
30. **Lee, C. H., et al.** 2005. Identification of the heterogeneous nuclear ribonucleoprotein A2/B1 as the antigen for the gastrointestinal cancer specific monoclonal antibody MG7. Proteomics **5:**1160–1166.
31. **Lee, C. L., et al.** 2003. Strategic shotgun proteomics approach for efficient construction of an expression map of targeted protein families in hepatoma cell lines. Proteomics **3:**2472–2486.
32. **Lescar, J., and B. Canard.** 2009. RNA-dependent RNA polymerases from flaviviruses and Picornaviridae. Curr. Opin. Struct. Biol. **19:**759–767.
33. **Levesque, K., et al.** 2006. Trafficking of HIV-1 RNA is mediated by heterogeneous nuclear ribonucleoprotein A2 expression and impacts on viral assembly. Traffic **7:**1177–1193.
34. **Limjindaporn, T., et al.** 2007. Sensitization to Fas-mediated apoptosis by dengue virus capsid protein. Biochem. Biophys. Res. Commun. **362:**334–339.
35. **Lin, J. Y., et al.** 2008. Heterogeneous nuclear ribonuclear protein K interacts with the enterovirus 71 5′ untranslated region and participates in virus replication. J. Gen. Virol. **89:**2540–2549.
36. **Lin, J. Y., et al.** 2009. hnRNP A1 interacts with the 5′ untranslated regions of enterovirus 71 and Sindbis virus RNA and is required for viral replication. J. Virol. **83:**6106–6114.
37. **Lin, R. J., B. L. Chang, H. P. Yu, C. L. Liao, and Y. L. Lin.** 2006. Blocking of interferon-induced Jak-Stat signaling by Japanese encephalitis virus NS5 through a protein tyrosine phosphatase-mediated mechanism. J. Virol. **80:**5908–5918.
38. **Lindenbach, B. D., and C. M. Rice.** 2003. Molecular biology of flaviviruses. Adv. Virus Res. **59:**23–61.
39. **Ma, L., C. T. Jones, T. D. Groesch, R. J. Kuhn, and C. B. Post.** 2004. Solution structure of dengue virus capsid protein reveals another fold. Proc. Natl. Acad. Sci. U. S. A. **101:**3414–3419.
40. **Mackenzie, J. M., and E. G. Westaway.** 2001. Assembly and maturation of the flavivirus Kunjin virus appear to occur in the rough endoplasmic reticulum and along the secretory pathway, respectively. J. Virol. **75:**10787–10799.
41. **Majumder, M., et al.** 2009. The hnRNA-binding proteins hnRNP L and PTB are required for efficient translation of the Cat-1 arginine/lysine transporter mRNA during amino acid starvation. Mol. Cell. Biol. **29:**2899–2912.
42. **Makino, Y., et al.** 1989. Detection of dengue 4 virus core protein in the nucleus. II. Antibody against dengue 4 core protein produced by a recombinant baculovirus reacts with the antigen in the nucleus. J. Gen. Virol. **70:**1417–1425.
43. **Marusawa, H., M. Hijikata, T. Chiba, and K. Shimotohno.** 1999. Hepatitis C virus core protein inhibits Fas- and tumor necrosis factor alpha-mediated apoptosis via NF-kappaB activation. J. Virol. **73:**4713–4720.
44. **Miller, S., S. Kastner, J. Krijnse-Locker, S. Buhler, and R. Bartenschlager.** 2007. The non-structural protein 4A of dengue virus is an integral membrane protein inducing membrane alterations in a 2K-regulated manner. J. Biol. Chem. **282:**8873–8882.
45. **Miller, S., and J. Krijnse-Locker.** 2008. Modification of intracellular membrane structures for virus replication. Nat. Rev. Microbiol. **6:**363–374.
46. **Misra, U. K., and J. Kalita.** 2010. Overview: Japanese encephalitis. Prog. Neurobiol. **91:**108–120.
47. **Moran-Jones, K., J. Grindlay, M. Jones, R. Smith, and J. C. Norman.** 2009. hnRNP A2 regulates alternative mRNA splicing of TP53INP2 to control invasive cell migration. Cancer Res. **69:**9219–9227.
48. **Mori, Y., et al.** 2005. Nuclear localization of Japanese encephalitis virus core protein enhances viral replication. J. Virol. **79:**3448–3458.
49. **Mori, Y., et al.** 2007. Processing of capsid protein by cathepsin L plays a crucial role in replication of Japanese encephalitis virus in neural and macrophage cells. J. Virol. **81:**8477–8487.
50. **Netsawang, J., et al.** 2010. Nuclear localization of dengue virus capsid protein is required for DAXX interaction and apoptosis. Virus Res. **147:**275–283.
51. **Noisakran, S., et al.** 2008. Identification of human hnRNP C1/C2 as a dengue virus NS1-interacting protein. Biochem. Biophys. Res. Commun. **372:**67–72.
52. **Nugent, C. I., K. L. Johnson, P. Sarnow, and K. Kirkegaard.** 1999. Functional coupling between replication and packaging of poliovirus replicon RNA. J. Virol. **73:**427–435.
53. **Oh, W., et al.** 2006. Jab1 mediates cytoplasmic localization and degradation of West Nile virus capsid protein. J. Biol. Chem. **281:**30166–30174.
54. **Oh, W. K., and J. Song.** 2006. Hsp70 functions as a negative regulator of West Nile virus capsid protein through direct interaction. Biochem. Biophys. Res. Commun. **347:**994–1000.
55. **Paranjape, S. M., and E. Harris.** 2007. Y box-binding protein-1 binds to the dengue virus 3′-untranslated region and mediates antiviral effects. J. Biol. Chem. **282:**30497–30508.
56. **Patkar, C. G., and R. J. Kuhn.** 2008. Yellow fever virus NS3 plays an essential role in virus assembly independent of its known enzymatic functions. J. Virol. **82:**3342–3352.
57. **Quaresma, A. J., et al.** 2009. Human hnRNP Q re-localizes to cytoplasmic granules upon PMA, thapsigargin, arsenite and heat-shock treatments. Exp. Cell Res. **315:**968–980.
58. **Ruggieri, A., T. Harada, Y. Matsuura, and T. Miyamura.** 1997. Sensitization to Fas-mediated apoptosis by hepatitis C virus core protein. Virology **229:**68–76.
59. **Shan, J., T. P. Munro, E. Barbarese, J. H. Carson, and R. Smith.** 2003. A molecular mechanism for mRNA trafficking in neuronal dendrites. J. Neurosci. **23:**8859–8866.
60. **Shi, S. T., G. Y. Yu, and M. M. Lai.** 2003. Multiple type A/B heterogeneous nuclear ribonucleoproteins (hnRNPs) can replace hnRNP A1 in mouse hepatitis virus RNA synthesis. J. Virol. **77:**10584–10593.
61. **Sumiyoshi, H., et al.** 1987. Complete nucleotide sequence of the Japanese encephalitis virus genome RNA. Virology **161:**497–510.
62. **Tsuda, Y., et al.** 2006. Nucleolar protein B23 interacts with Japanese encephalitis virus core protein and participates in viral replication. Microbiol. Immunol. **50:**225–234.
63. **van Marle, G., et al.** 2007. West Nile virus-induced neuroinflammation: glial infection and capsid protein-mediated neurovirulence. J. Virol. **81:**10933–10949.
64. **Wang, S. H., W. J. Syu, and S. T. Hu.** 2004. Identification of the homotypic interaction domain of the core protein of dengue virus type 2. J. Gen. Virol. **85:**2307–2314.
65. **Welsch, S., et al.** 2009. Composition and three-dimensional architecture of the dengue virus replication and assembly sites. Cell Host Microbe **5:**365–375.
66. **Westaway, E. G., A. A. Khromykh, M. T. Kenney, J. M. Mackenzie, and M. K. Jones.** 1997. Proteins C and NS4B of the flavivirus Kunjin translocate independently into the nucleus. Virology **234:**31–41.
67. **Westaway, E. G., J. M. Mackenzie, and A. A. Khromykh.** 2003. Kunjin RNA replication and applications of Kunjin replicons. Adv. Virus Res. **59:**99–140.
68. **Westaway, E. G., J. M. Mackenzie, and A. A. Khromykh.** 2002. Replication and gene function in Kunjin virus. Curr. Top. Microbiol. Immunol. **267:**323–351.
69. **Wiwanitkit, V.** 2009. Development of a vaccine to prevent Japanese encephalitis: a brief review. Int. J. Gen. Med. **2:**195–200.
70. **Yang, J. S., et al.** 2002. Induction of inflammation by West Nile virus capsid through the caspase-9 apoptotic pathway. Emerg. Infect. Dis. **8:**1379–1384.
71. **Yang, M. R., et al.** 2008. West Nile virus capsid protein induces p53-mediated apoptosis via the sequestration of HDM2 to the nucleolus. Cell. Microbiol. **10:**165–176.
72. **Yan-Sanders, Y., G. J. Hammons, and B. D. Lyn-Cook.** 2002. Increased expression of heterogeneous nuclear ribonucleoprotein A2/B1 (hnRNP) in pancreatic tissue from smokers and pancreatic tumor cells. Cancer Lett. **183:**215–220.
73. **Yao, Z., et al.** 2010. B23 acts as a nucleolar stress sensor and promotes cell survival through its dynamic interaction with hnRNPU and hnRNPA1. Oncogene **29:**1821–1834.
74. **Yu, F., F. Hasebe, S. Inoue, E. G. Mathenge, and K. Morita.** 2007. Identification and characterization of RNA-dependent RNA polymerase activity in recombinant Japanese encephalitis virus NS5 protein. Arch. Virol. **152:**1859–1869.
75. **Zhou, J., et al.** 2001. Differential expression of the early lung cancer detection marker, heterogeneous nuclear ribonucleoprotein-A2/B1 (hnRNP-A2/B1) in normal breast and neoplastic breast cancer. Breast Cancer Res. Treat. **66:**217–224.

Virology 412 (2011) 211–219

Contents lists available at ScienceDirect

Virology

journal homepage: www.elsevier.com/locate/yviro

Involvement of cyclophilin B in the replication of Japanese encephalitis virus

Hiroto Kambara, Hideki Tani, Yoshio Mori, Takayuki Abe, Hiroshi Katoh, Takasuke Fukuhara, Shuhei Taguwa, Kohji Moriishi, Yoshiharu Matsuura *

Department of Molecular Virology, Research Institute for Microbial Diseases, Osaka University, 3-1 Yamada-oka, Suita, Osaka 565-0871, Japan

ARTICLE INFO

Article history:
Received 15 November 2010
Returned to author for revision
19 December 2010
Accepted 7 January 2011
Available online 1 February 2011

Keywords:
JEV
Cyclophilin B
Cyclosporine A
Replication

ABSTRACT

Japanese encephalitis virus (JEV) is a mosquito-borne RNA virus that belongs to the *Flaviviridae* family. In this study, we have examined the effect of cyclosporin A (CsA) on the propagation of JEV. CsA exhibited potent anti-JEV activity in various mammalian cell lines through the inhibition of CypB. The propagation of JEV was impaired in the CypB-knockdown cells and this reduction was cancelled by the expression of wild-type but not of peptidylprolyl *cis-trans* isomerase (PPIase)-deficient CypB, indicating that PPIase activity of CypB is critical for JEV propagation. Infection of pseudotype viruses bearing JEV envelope proteins was not impaired by the knockdown of CypB, suggesting that CypB participates in the replication but not in the entry of JEV. CypB was colocalized and immunoprecipitated with JEV NS4A in infected cells. These results suggest that CypB plays a crucial role in the replication of JEV through an interaction with NS4A.

Introduction

The genus *Flavivirus* within the family *Flaviviridae* comprises over 70 viruses, many of which are predominantly arthropodborne viruses, such as Japanese encephalitis virus (JEV), West Nile virus (WNV), Murray Valley encephalitis virus, dengue virus (DENV), yellow fever virus (YFV), and tick-borne encephalitis virus. JEV is one of the most important flaviviruses in the medical and veterinary fields and exists in a zoonotic transmission cycle among mosquitoes, pigs, and birds mostly in Eastern and Southeast Asia. This virus spreads to dead-end hosts, including humans, through the bite of JEV-infected mosquitoes, and around 30,000–50,000 cases and up to 15,000 deaths are reported annually (Ghosh and Basu, 2009; Mackenzie et al., 2004; Solomon et al., 2003). JEV has a single-stranded positive-sense RNA genome of approximately 11 kb, which is capped at the 5′ end but lacks a 3′ polyadenine tail. The genome RNA is translated into a single large polyprotein at the endoplasmic reticulum (ER) membrane, then cleaved by the host- and virus-encoded proteases into three structural proteins, the capsid, precursor membrane (prM), and envelope (E) proteins, and seven nonstructural (NS) proteins, NS1, NS2A, NS2B, NS3, NS4A, NS4B, and NS5 (Sumiyoshi et al., 1987).

Flavivirus infection causes extensive rearrangement of cellular membranes to form two distinct membrane structures called the vesicle packet and convoluted membrane (Mackenzie et al., 1996; Miller and Krijnse-Locker, 2008). Whereas the vesicle packet is believed to contain the replication complex in which viral RNA synthesis takes place, the convoluted membrane is the putative site for viral polyprotein processing (Mackenzie et al., 1999). A recent tomography study clarified that the ER, convoluted membrane, and outer membrane of the vesicle packet were connected together to form a continuous membrane, with the vesicle packet being observed as an invagination of the ER with NS proteins and viral RNA, suggesting that viral replication occurred on the surface of the ER (Welsch et al., 2009). The structures of the convoluted membrane can be observed by infection with the WNV strain Kunjin virus or expression of the DENV NS4A protein alone (Miller et al., 2007; Roosendaal et al., 2006). Previous studies have indicated that NS4A localizes to both the vesicle packet and convoluted membrane and interacts with NS1, indicating that NS4A plays an important role as an integral scaffold of the replication complex (Lindenbach and Rice, 1999; Mackenzie et al., 1998).

In addition to NS proteins, flavivirus RNA replication is known to be regulated by several host factors, such as eEF1A, TIA/TIAR, HMGCR, and cyclophilin (Cyp) A (Davis et al., 2007; Emara and Brinton, 2007; Mackenzie et al., 2007; Qing et al., 2009). RNAi screening has identified various host factors involved in the replication of RNA viruses, including the hepatitis C virus (HCV), human immunodeficiency virus (HIV), and influenza A virus (Karlas et al., 2010; Konig et al., 2010, 2008; Tai et al., 2009). Host factors essential for viral replication might be an ideal target for antiviral development because the frequency of appearance of resistant viruses is lower by this method than when using antivirals targeted to the viral proteins.

In this study, we identified CypB as a host factor involved in the propagation of JEV. CypB is a member of the Cyp family, is ubiquitously expressed in most cells, and predominantly resides in the ER through the ER retention signal sequence in the C-terminus (Price et al., 1994,

* Corresponding author. Fax: +81 6 6879 8269.
E-mail address: matsuura@biken.osaka-u.ac.jp (Y. Matsuura).

0042-6822/$ – see front matter © 2011 Elsevier Inc. All rights reserved.
doi:10.1016/j.virol.2011.01.011